Table 6 Result of dating by K–Ar method

Sample No.	(1) K %	(2) ^{40}K 10^{-4}%	(3) ^{40}Ar cc/gx10^{-5}	(4) ^{40}Ar g/gx10^{-8}	(5) ^{40}Ar 10^{-6}%	(6) $^{40}Ar/^{40}K$ 10^{-2}	(7) Age 10^6 years	(8) Ave. Age 10^6 years	(9) σ 10^6 years	(11) Rad ^{40}Ar %
25-1-1	2.72	3.247	9.95	17.76	17.76	5.470	757.5	734.7	18.1	98.5
	2.66	3.176	9.03	16.11	16.11	5.072	711.9			98.2
28A-109	0.66	0.788	2.04	3.64	3.64	4.619	658.6	662.8	16.4	92.7
	0.67	0.800	2.10	3.75	3.75	4.688	666.9			95.5
22-6	1.97	2.352	5.96	10.63	10.63	4.520	646.7	640.2	16.4	89.9
	1.95	2.328	5.79	10.34	10.34	4.442	633.6			88.6
27-A-105	9.43	11.26	25.94	46.31	46.31	4.113	597.1	576.7	14.2	98.8
	9.48	11.32	24.00	42.84	42.84	3.785	556.2			98.6
22-2	3.75	4.478	9.17	16.37	16.37	3.656	539.8	537.5	13.4	90.5
	3.74	4.466	9.06	16.17	16.17	3.621	535.2			90.6

25-1-1 : Garnet bearing muscovite biotite gneiss

28A-109: Hornblende gneiss

22-6 : Muscovite biotite granodiorite

27A-105: Perthite in pegmatite

22-2 : Hornblende adamellite

$$T = \frac{1}{\lambda} \ln\left(1 + \frac{\lambda}{\lambda e} \cdot \frac{^{40}Ar}{^{40}K}\right)$$

T = time

λ_β = disintegration constant from ^{40}K to ^{40}Ca

λ_e = disintegration constant from ^{40}K to ^{40}Ar

λ = total constant

The constants for the age calculation are : $\lambda_\beta = 4.962 \times 10^{-10}\ yr^{-1}$,

$\lambda e = 0.581 \times 10^{-10}\ yr^{-1}$, $^{40}K = 1.167 \times 10^{-4}$ atom per atom of natural potassium.

(Convention on decay constants, Subcommission on Geochronology, 25th International Geological Congress, 1976)

(1), (3) and (11) were measured. (4) was calculated by (3) x 40g/22410cc = (3) x 1.785×10^{-3}

(2) was calculated by (1) x $1.167 \times 10^4 \times \frac{40}{39.1}$ = (1) x 1.194×10^{-4} (9) is standard deviation

$$\sigma = \left[\sigma_k^2 + \sigma_x^2 + \sigma^2_{40/38}\left(\frac{1}{\gamma}\right)^2 + \sigma^2_{36/38}\left(\frac{1-\gamma}{\gamma}\right)^2\right]^{1/2}$$

σ_k = standard deviation of K

σ_x = standard deviation of calibration for tracer ^{38}Ar

$\sigma_{40/38}$ = standard deviation of ratio of $^{40}Ar/^{38}Ar$ of Mass spectrometer measurement

$\sigma_{38/36}$ = ditto $^{38}Ar/^{36}Ar$ ditto

γ = ratio of radiogenic ^{40}Ar to total ^{40}Ar

The following parameters are held in general in this experiment.

$\sigma_k = 1\%$ $\sigma_x = 2\%$ $\sigma_{40/38} = 1\%$ $\sigma_{38/36} = 2\%$

2–8–1 Metallic Mineral Deposits

1) Wadi Shaat

A lead mineral showing in an old trench is located about 13 km northwestward from Sadh at 100 m in altitude, near the field camp. It occurs in a acidic dyke in the Juffa gneiss as veinlet~network of galena and quartz running collectively in N 60° E strike and vertical dip. Tiny cubic crystals of galena are observable and under the reflecting microscope, only galena is identified (Photomicrograph 37). The result of chemical analysis on a sample (No. 25–5) of 5 cm in size shows 33.66 % Pb, <0.01 % Zn, 0.2 g/t Au and 6 g/t Ag. Though the grade of lead is high, it is thought that the continuity of mineralized zone may not be expected owing to the very small scale of mineral showing zone.

2) Wadi Morir

Dark brown, cubic crystals up to 7 cm occur associated with pegmatite in the Sadh gneiss on Wadi Morir about 9 km northeastward from Sadh. Only hematite is identified by X–ray powder patterns (X–ray chart 1). Hematite is altered from pyrite that remains at the central part of the crystals.

3) Wadi Hadabin

A gravel with gossan was collected by a boy at the Hadabin village.
It occurs on a tributary of Wadi Hadabin near the coast southwestward from Jabal Nuss at 50 m in altitude, located about 22 km northeastward from Sadh. The sample is megascopically composed of pegmatite accompanying pyrite, hematite and limonite associated with quartz, and only the hematite and goethite are identified by X–ray powder diffractions applied only to the part of samples containing secondary minerals (X–ray chart 2).

4) Wadi Kohrhant

Many pegmatites 2~3-m-thick run in NNW–SSE strike about 4 km westward from Sadh, including malachite, limonite and pyrite. Limonite composed of goethite occurs dominantly in size of the lemon to bean. Malachite is light green and forms thin film associated with limonite. These ore minerals occur randomly as aggregates 10 cm in diameter in the upper, middle and lower parts of the pegmatite. Malachite is faintly confirmed by X–ray powder patterns (X–ray chart 3) and the grade of Cu is low at 0.32 % as the result of chemical analysis of a sample including malachite.

Such first confirmation of malachite occurrence is very important for future exploration in the area.

5) Ras Ayn

Pyrrhotite and pyrite on the hanging wall side of pegmatite occur as vein partly as lens of 10 cm x 15 cm in size in the Sadh gneiss about 19 km eastward from Mirbat.
The result of chemical analysis shows 37.37 % Fe and < 0.01 % Cu. Also, under the reflecting microscope any other ore minerals than pyrrhotite and pyrite cannot be found.

As mentioned above, a small amount of pyrite, pyrrhotite, galena, hematite, malachite and limonite have been observed in serveral locations and these are thought to be accompanied with pegmatite and hydrothermal vein. Pegmatite minerals such as rare earth and Nb–Ta minerals have not yet been found.

2–8–2 Uranium

Radioactive measurement was carried out simultaneously with ground surface geological survey. Radioactivities were measured with Aloka γ–ray scintitation surveymeter made in Japan by total γ–radiation of U, Th and K. The background value of the surveymeter was always 5 μr/hr in Salalah and the two field camps. Radioactivities were continuously measured on each exposure by about ten-second time-constant.

The result of radioactive measurements during helicopter and surface surveys in shown in Table 7, and, especially in Figs. 15 and 16, the result from the two parts of the Mirbat sandstone formation is shown together with geologic columnar sections. The reason why the Mirbat sandstone formation were surveyed in detail is based on the fact mentioned below:

a) The formation is only one formation composed of clastic material such as conglomerate, sandstone, siltstone and shale in the surveyed area and is gently inclined overlying the Precambrian basement unconformably, which is generally thought to make a favorable condition for uranium depostion.

b) Radioactivity three times of the background value, that is, 15 μr/hr, was detected on siltstone at the mountain side of Jabal Shereef during the helicopter survey carried out on the first day.

1) Precambrian basement

Each of the measured radioactivity represents the difference of each rock type of the Precambrian basement.

The garnet bearing muscovite-biotite gneiss shows the value generally over 10 μr/hr and the hornblende gneiss shows about 5 μr/hr similar to the background value. This difference distinctively appears at the contact part of the both gneisses, for instance, at the point close to the 25–1 and 28–A–109 located near Wadi Shaat about 10 km northwestward from Jabal Qinquari. This difference is due to the differences of mineral component and chemical composition in each rock type.

Muscovite-biotite-magnetite gneiss occurs in the hornblende gneiss belonging to the Sadh gneiss though an exact relation between the both is obsecure.

The gneiss is distributed on the left bank of the mouth of Wadi Ayn. It is composed of each 1 ~ 3-cm-thick, black and pink bands elongating about 10 m with 0.5 ~ 1.0 m thickness (Photo. 11). Mineral component is rather granitic under the microscope (Photomicrographs 5.6). The result of chemical analysis shows 0.003 % U_3O_8 and 0.001 % ThO_2.

Table 7 Result of radioactive measurements at the Salalah area

Location	Lithology	μr/hr	Remarks
22–1	Limestone	5	Late Cretaceous ~ Early Tertiary
22–2	Hornblende adamellite (stock)	14 ~ 15	
22–3	Muscovite biotite quartz diorite	10	
	Pegmatite (dyke)	6 ~ 7	
	Sandstone	10	Late Cretaceous ~ Early Tertiary
22–5	Trondhjemite (dyke)	4	
	Biotite hornblende quartz diorite	2	
22–6	Muscovite biotite gradodiorite	6 ~ 8	
22–7	Gravel, sand	5 ~ 6	Raised beach
22–8	Biotite muscovite magnetite gneiss	33 ~ 35	Granodioritic
	Pegmatite (dyke)	14 ~ 15	
22–9	Siltstone	15	Mirbat sandstone
	Medium-grained sandstone	8 ~ 9	ditto
22–10	Coarse-grained arkose sandstone	6 ~ 10	ditto
25– 1	Muscovite biotite gneiss	15	Quartz dioritic
	Hornblende gneiss	5	Intercalation in biotite gneiss
25– 2	Muscovite biotite gneiss	6	Quartz dioritic
	Dolerite (dyke)	5	
25– 3	Granophyre (dyke)	15 ~ 20	Carbonitization, epidotization
	Muscovite biotite gneiss	15 ~ 20	
25– 4	ditto	15	
25– 5	Microdiorite? (dyke)	10	Host rock of lead mineralization
26–A–101	Hornblendite	2	
	Serpentinite	5	
26–B–101	Quartz porphyry (dyke)	21 ~ 24	Sericitization, carbonitization
〃	Dolerite (dyke)	13	ditto
	Quartz diorite	12	
104	Muscovite biotite gneiss	13	
27–A–101	Hornblendite	4	Xenolith in granodiorite
	Granodiorite	5	
27–A–103	Gneissose biotite quartz diorite	8	
27–A–105	Pegmatite (dyke)	13 ~ 15	
28–A–101	Biotite hornblende gneiss	8	Quartz dioritic
28–A–102	Hornblende gneiss	5	Dioritic
28–A–103	Hornblende gneiss	5	Quartz dioritic
28–A–104	Gneissose hornblende quartz diorite	5	
28–A–106	Pegmatite (dyke)	6	
28–A–109	Hornblende gneiss	5	Quartz dioritic
	Biotite gneiss	10	
28–A–110	Hornblende gneiss	3	Quartz dioritic
28–A–111	Gneissose hornblende gabbro	5	

Note: Radioactivity was measured with Aloka γ-ray scintilation survey meter (Type TCS–121C).

The Quartz diorite~granodiorite batholith (Nos. 22–3, 22–5 and 22–6) and small bodies of quartz-diorite show the radioactivity of 4 ~ 12 μr/hr.

Pegmatite shows 6 ~ 15 μr/hr in the four locations. Potash feldspar and/or biotite bearing part shows generally higher radioactivity. The part showing 15 μr/hr is due to biotite and pink potash feldspar.

Dolerite shows 5 μr/hr and 13 μr/hr in the two locations. At the 26–B–101 point, 1.5-m-thick dolerite dyke occurs between about 1.5-m-thick garnet bearing muscovite-biotite gneiss showing 13 μr/hr and 2 to 3 m thick quartz porphyry dyke showing 21 ~ 24 μr/hr. Radioactivity, 15 μr/hr of this dolerite dyke, is thought to have been raised by the effect of radioactivity of the surrounding gneiss and quartz porphyry dyke.

Quartz porphyry dyke shows 15 μr/hr and 24 μr/hr in the two locations and the adamellite stock shows 14 ~ 15 μr/hr. These values are more than three times of the background value.

As mentioned above, radioactivity is increased in the order of dolerite, hounblende gneiss~quartz diorite gneiss (Sadh gneiss), quartz diorite and granodiorite, garnet bearing muscovite-biotite gneiss (Juffa gneiss) and adamellite stock~quartz porphyry dyke.

2) Mirbat sandstone formation

The result of radioactive measurements is shown in the second rightest column in Figs. 14 and 15.

Muscovite-quartz diorite of the Precambrian basement shows 5 μr/hr same as background value. Concerning the Lower member, coarse- to fine-grained sandstone 40 m thick shows generally 5 ~ 7 μr/hr, though an alternation of medium- and fine-grained sandstones each 2-m-thick with intercalations of siltstone shows 12 ~ 15 μr/hr. In the alternative zone in the part from 50 m to 57.5 m in the column in Figs. 14, 15 of silty sandstone~siltstone 50-cm-thick and medium-grained sandstone 20-cm-thick, the siltstone shows 9 ~ 12 μr/hr and the medium-grained sandstone 6 ~ 8 μr/hr respectively.
Also, in the similar alternation zone 7-m-thick in the upper part from 70 m, the siltstone shows 12 ~ 16 μr/hr and the medium-grained sandstone 12 ~ 14 μr/hr.

On the other hand, in the upper part of the Middle member, the medium-grained sandstone shows the value generally under 10 μr/h. In a 4-m-thick alternation zone of medium-grained sandstone and siltstone from 53 m to 57 m the snadstone shows 8 μr/hr and siltstone 14 μr/hr. Fine-grained sandstone and siltstone often accompanied by shale, show 10 ~ 15 μr/hr, though the former has generally lower value than the latter. Also, an alternative zone of siltstone and shale with intercalations of under 5-cm-thcik fine-grained sandstone, constituting the lowermost of the Upper member, shows 10 ~ 14 μr/hr.

As mentioned above, radioactivity of medium~coarse-grained sandstone is generally lower than 10 μr/hr and that of siltstone and shale is higher at 10 ~ 15 μr/hr.

The result of chemical analysis of the siltstone sample (No. 22–9) collected at the mountain side of Jabal Shereef during the first-day helicopter survey shows 0.004 % U_3O_8, and this is about ten times value compared with that of common siltstone. Under the microscope, it is mostly composed of quartz grains of 0.1~0.01 mm in size, and a small amount of muscovite flakes under 0.1 mm in size and tiny spherical limonite are discriminated (Photomicrographs 31. 32). X–ray powder diffraction patterns of the fine fraction obtained by hydraulic classifying shows that the fraction is composed of sericite, kaolinite and quartz (X–ray chart 4). Uranium is thought to be adsorbed by clay minerals such as sericite and kaolinite.

3) Umm er Radhuma formation

Radioactivity was measured only in two locations during the helicopter survey, because it is distributed in the upper part of the escarpment. No. 22–2 is limestone and shows 5 μr/hr, and No. 22–3 is sandstone and shows 10 μr/hr. Limestone near No. 22–3 shows always 5 μr/hr.

4) Quaternary sediments

Wadi sediments and raised beach show always about 5 μr/hr.

The radioactive anomaly near the air strip of Juffa Camp reported by Mackay and Schnellman Ltd. (1977) could not be detected. The raised beach plateau of Juffa Camp shows always 5 μr/hr even near an old sampling pit, samples from which were reported to contain 18 to 21 ppm U_3O_8. In this old pit, radioactivity is 5 ~ 6 μr/hr. It is supposed that all radioactive gravels were collected at the previous survey.

2–8–3 Other Minerals

Quartz and feldspar are abundant, because many quartz veins and pegmatite are distributed in the Precambrian basement. Some parts of quartz and feldspar are of available grade for ceramic use but it is doubtful that they are economically operated. Also, a quartz porphyry dyke seems to be suitable for ceramic use as pottery stone, because it is almost wholly composed of quartz and sericite, though iron content is rather high.

Asbestos occurs partly in the basic gneiss but is not of econimic use.

2–9 Geochemical Exploration

The area belongs to an arid zone without rainfall except the monsoon season from June to September and geochemical exploration by soil is not applicable owing to scantiness of soil formation on the ground surface. The initial purpose of geochemical exploration was to collect test samples throughout the whole area for investigating whether geochemical exploration by wadi sediments is applicable or not and finding out most favorable sampling point on wadi. But, the fact that geochemical exploration of wadi sediments had been already carried out throughout the whole area by Woodrow-Towell Co. was informed after arrival in Oman. In this geochemical exploration, samples under 80 mesh were collected at the rate of one sample to one square kilometer, and only very weak anomalies for

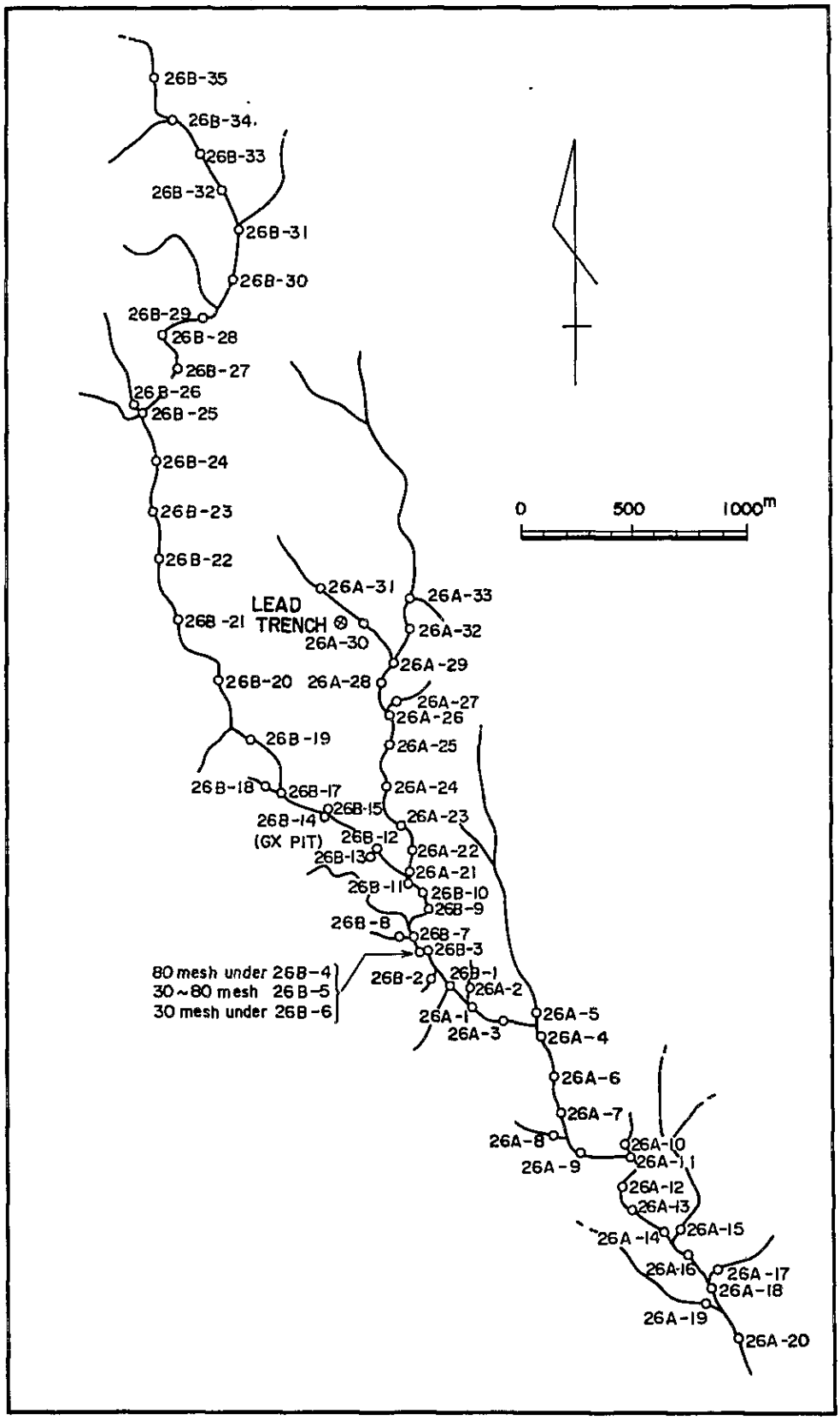

Fig. 17 Location map of stream sediment samples near old lead trench

Pb,Cu, Cr, Sb, etc. were confirmed.

Accordingly, the initial plan was changed to two ways of sampling as follows:

1) 150 ~ 200 m interval sampling, which is denser than that of T.W.T., on the narrow Wadi eastward from Wadi Shaat, where an old lead pit is present and also weak anomalies for Sb and Cr were confirmed, to detect anomalies suggesting the lead mineralization and to examine the variation of Cu, Pb and Zn in more detail.

2) 10 ~ 20 m interval sampling across broad wadis to examine variation by sampling points.

2–9–1 Sampling Location

An old lead pit is located about 2 km eastward from the field camp site, but, any lead anomaries could not be confirmed by geochemical exploration of T.W.T..
The sampling map at this time is shown in Fig. 17.

On Wadi Mahall and Wadi Shaat, sampling across wadi bed each 10 ~ 20 m interval was carried out. Also, a few samples were collected near gossan exposure or float on Wadi Khorhanfa, Wadi Hadabin, etc..

2–9–2 Sampling Method

Samples were collected from the points supposed to be stream bed during the monsoon period and if a tributary is present, two samples, one from the tributary and another from the confluence in main wadi were collected.

It was very difficult to collect enough samples under 80 mesh for chemical analysis because of the coarse-grained constituents, and samples under 30 mesh are sieved immediately after their collection.

The collected sample, which was put into vinyl sample bag, was sent to Japan and then analysed.

2–9–3 Analytical Method

Ten samples were qualitatively analyzed by emission spectrochemical analysis to determine chemical elements suitable for geochemical exploration. From the result shown in Table 8, main base metal elements are generally scanty and weak in variation, but, Cu, Pb and Ti show some variation. Therefore, the four compositions adding Zn to the three are quantitatively analyzed. Pb, Zn and Cu are analyzed on the whole samples by atomic absorption method and Ti are analyzed on several samples by colorimetric method.

1) Atomic absorption method

One gram sample is analyzed through the following process after pulverizing under 100 mesh.

Samples → + 20 ml aqua regia (HCl 3: HNO_3 1: H_2O 1) + 5 ml HCl → Heating untill generation of white hume, distilling and drying on sand bath → Air cooling → + 8 ml HCl (1 : 1) → Heating and dissolving → Air cooling → Adjusting to 20 ml solution with H_2O.

Table 8 Emission spectrochemical analysis

Composition / Sample No.	Ag	B	Co	Cr	Cu	K	Mg	Mn	Mo	Na	Ni	Pb	Sb	Sn	Ti	V	Zn
26–A– 1	–	–	–	1	1	4	3	1	–	5	0	–	–	–	3	1	–
26–A–10	–	–	–	1	1	4	4	2	–	5	1	–	–	–	3	1	–
26–A–20	–	–	–	1	0	4	3	1	–	5	0	–	–	–	3	1	–
26–A–30	–	–	–	1	0	4	4	2	–	5	0	0	–	–	3	1	–
26–B–10	–	–	–	1	0	4	3	1	–	5	0	–	–	–	3	1	–
26–B–20	–	–	–	1	0	4	3	1	–	5	0	–	–	–	3	1	–
26–B–30	–	–	–	1	0	4	3	1	–	5	0	–	–	–	3	1	–
26–B–35	–	–	–	1	0	4	3	1	–	5	0	–	–	–	3	1	–
27–A– 3	–	–	–	1	0	4	3	1	–	5	0	–	–	–	3	1	–
27–A–25	–	–	–	1	0	4	3	1	–	5	0	–	–	–	3	1	–

Al, Fe, Si : all sample 5

– : nil
0 : feeble
1 : very weak
2 : weak
3 : medium
4 : strong
5 : very strong

Analysis condition

Quartz prism spectro-camera : intermediate focus method, 10 μm slit

Electric power : D.C 280V, 5A, continuous arc, 30 sec. exposure

Film : Din 19, 20°C 5 min. develop

Table 9 Metal content of stream sediments

Ser. No.	Sample No.	Cu ppm	Pb ppm	Zn ppm	Ti %	Ser. No.	Sample No.	Cu ppm	Pb ppm	Zn ppm	Ti %
1	26-A-1	21	6	44	–	51	26-B-18	25	6	53	–
2	2	23	6	55	–	52	19	19	3	37	–
3	3	18	6	50	–	53	20	23	3	38	–
4	4	27	6	42	–	54	21	19	3	39	0.12
5	5	26	3	55	–	55	22	19	0	44	–
6	6	15	3	34	–	56	23	21	6	43	–
7	7	18	6	35	–	57	24	30	6	40	–
8	8	29	3	52	–	58	25	19	3	34	–
9	9	35	6	41	–	59	26	24	10	49	–
10	10	26	3	54	–	60	27	20	0	39	–
11	11	20	3	35	0.11	61	28	20	0	38	–
12	12	15	3	34	–	62	29	25	0	38	–
13	13	19	6	31	–	63	30	16	0	32	–
14	14	19	6	39	–	64	31	21	0	41	0.13
15	15	19	6	45	–	65	32	20	0	35	–
16	16	14	6	32	–	66	33	15	3	34	–
17	17	25	10	64	–	67	34	24	3	45	–
18	18	22	13	36	–	68	35	16	3	34	–
19	19	18	13	49	–	69	27-A-1	3	3	21	–
20	20	17	10	46	0.16	70	2	5	3	25	–
21	21	17	10	32	–	71	3	11	3	39	–
22	22	19	6	43	0.19	72	4	4	0	25	–
23	23	21	10	49	–	73	5	3	0	19	–
24	24	17	3	32	–	74	6	13	3	56	–
25	25	22	10	45	–	75	7	13	0	35	–
26	26	19	6	39	–	76	8	15	0	47	–
27	27	27	9	60	–	77	9	21	3	34	–
28	28	21	6	47	–	78	10	16	3	27	–
29	29	19	6	52	0 20	79	11	22	3	36	–
30	30	29	20	55	–	80	12	25	3	37	–
31	31	34	13	60	–	81	13	22	3	41	–
32	32	29	6	44	–	82	14	21	3	43	–
33	33	22	3	46	–	83	15	20	3	36	–
34	26-B-1	30	3	41	0.17	84	16	21	3	43	–
35	2	18	6	45	–	85	17	37	3	56	–
36	3	22	6	36	–	86	18	20	3	45	–
37	4	18	12	39	–	87	19	22	3	57	–
38	5	17	6	43	–	88	20	23	3	44	–
39	6	17	6	48	–	89	21	16	0	48	–
40	7	22	6	37	–	90	22	18	3	52	–
41	8	25	6	39	–	91	23	19	3	50	–
42	9	17	3	38	–	92	24	55	6	52	–
43	10	17	3	36	–	93	25	17	3	53	–
44	11	17	3	36	–	94	26	19	3	54	–
45	12	15	3	34	–	95	27	19	3	47	–
46	13	29	12	57	–	96	28	20	6	56	–
47	14	19	6	44	–	97	29	22	6	65	–
48	15	19	6	47	–	98	30	23	6	56	–
49	16	21	10	46	–	99	28-A-1	16	6	43	–
50	17	19	6	40	–	100	2	18	0	47	–

Ser. No. 1 ~ 68 : east of Wadi Shaat
69 ~ 76 : West of Jabal Musayrah and Wadi Hadalsin
77 ~ 83 : Wadi Mahali
84 ~ 98 : Wadi Shaat
99 ~ 100: Wadi Khorhant

The solution is analyzed in wave length of 3,248Å for Cu, 2,833Å for Pb and 2,138Å for Zn.

b) Colorimetric method

Five grams sample is analyzed through the following process after pulverizing under 100 mesh.

Samples → + 20 ml HCl → Heating until distilling and drying on sand bath → Air Cooling → + 5 ml conc. HNO_3 → Repeating addition of 10 ~ 20 ml $HClO_4$ untill colorless state → Distilling with white hume on sand bath → Air cooling → + 30 ml H_2O → Heating and dissolving → Adjusting to 100 mg solution with 5 ml H_2PO_4, 5 ml $HClO_4$ and H_2O. The solution is analyzed with electric photometer in 420 mμ wave length.

2–9–4 Result

The result in Table 9 shows respectively a range from 3 ppm to 55 ppm for cupper, from 0 to 20 ppm for Pb, from 19 ppm to 65 ppm for Zn and from 0.11 % to 0.20 % for Ti. These values are thought to be generally low and not special as compared with common stream sediments in other districts in the world, and also, lower or similar as compared with Clark Number.

Pb content is generally low, but, the maximum value, 20 ppm, appears in the neigh bourhood of the old lead pit though the value at dowstream about 200 m is low as background value. The higher Pb content is thought to be reflected by the actual lead exposure.

Variation of metal content by 10 ~ 20 m intervals across Wadi Shaat seems to be small, though Cu content of one sample (Ser. No. 92) is rather high at 55 ppm. This sample was collected at rather higher portion of the wadi bed, and the reason for the high copper content is difficult to be explained.

Nos. 26–B–4, 26–B–5 and 26–B–6 are collected at the same point but separately in three, namely, under 80 mesh, 30 ~ 80 mesh and under 30 mesh. Each metal content shows almost no variation among the three samples.

As mentioned above, the result of geochemical exploration seems to suggest that whether the geochemical exploration by wadi sediments in the area is not effective or there is no remarkable base-metal mineralization.

2–10 Considerations

Data on geology and mineral deposit are very scanty as mentioned already. Only some recconnaisance surveys have been carried out up to the present.

Therefore, a fundamental survey to study general geology especially to decide geological succession has been carried out. Researches on mineral deposits and geochemical exploration also have been carried out.

1) Geological succession

The geological succession is as follows in ascending order:

a) Precambrian basement

Juffa gneiss —— mainly garnet bearing muscovite-biotite gneiss (734.7 ± 36.7 m.y.)

Sadh Gneiss —— Injection gneiss (hornblende gneiss and quartz diorite gneiss)
(662.8 ± 33.1 m.y.)

Quartz diorite, granodiorite —— batholith (640.2 ± 32.0 m.y.)

Pegmatite~quartz vein —— vein, network, lenticular
(576.7 ± 28.8 m.y.)

Stock and dyke —— hornblende adamellite stock (537.5 ± 26.9 m.y.),
and dolerite and quartz porphyry dykes

b) Ordovician Mirbat sandstone formation composed of Lower, Middle and Upper members, grain size of which increases from lower to upper.

c) Tertiary Umm er Radhuma formation composed mainly of limestone.

d) Quaternary sediments composed of raised beach, beach sand, aeolian sand due and wadi sediments.

The geological succession confirmed in this survey is almost similar to that of the Taylor Woodrow – Towell Co.. But it has been confirmed for the first time that (1) the overlying Sadh gneiss seems to have a gradual transitional contact to the underlying Juffa gneiss. (2) the Precambrian basement is surely Late Precambrian in age and the acidic dyke cuts the basic dyke.

2) Mineral showings

a) Metallic minerals

Copper, lead, etc. exposures are distributed in several locations though of a small scale associated with acidic dyke and pegmatite in the Precambrian basement.

It is desierable to carry out further survey for the discovery of mineralization in the distribution area of acidic dyke swarms and adamellite stocks and also in the surrounding area of quartz porphyry granodiorite batholith, though occurrence of large scale metallic mineral deposits related to submarine volcanism at the time of formation of original rocks of the gneiss might not be expected.

b) Uranium

Uranium has been detected at only one location in the Sadh gneiss, but, occurrence large scale uranium deposits such as quartz conglomerate type, anatectic type or vein type cannot be expected owing to the lithology of the Precambrian basement. Also, two- to three-fold radioactivity has been confirmed in siltstone beds of the Mirbat sandstone formation and only one analyzed sample contains 0.004 % U_3O_8 which is about ten times as that of common siltstone in the world.

It is desirable to carry out further survey for discovery of stronger uranium mineralization because the Mirbat sandstone formation is thought to be favorable for uranium deposit such as "Sandstone" type uranium deposit.

c) Geochemical exploration

Geochemical exploration has been carried out on wadi sediments almost wholly under 30 mesh because fine fractions enough for chemical analyses are very difficult to be collected. Generally, metal contents are very low and no variation of Cu, Pb and Zn due to the differences of the sampling locations and grain-sizes has been recognized. Only one lead anomaly has been confirmed near the old lead pit, but, at the downstream 200 m apart, an anomaly has not been detected.

Geochemical exploration is thought to be not suitable as a regional exploration method.

Chapter 3 Eastern Sur Area

Manganese ore deposits supposed to be of sedimentary origin are known in Khawr Jaramah. The Bureau of Minerals, Oman, carried out a brief study only on some parts of the deposits. Present study made a supplemental data for obtaining a general idea on the deposits, although the study was of a reconnaissance.

3–1 Location

The surveyed area is located about 25 km (in a straight line) east of Sur, a fishing port in the southeast to Muscat. Latitude and longitude of the area are $22^{\circ}22' \sim 22^{\circ}30'$ N and $39^{\circ}45' \sim 39^{\circ}50'$ E. (Fig. 18)

3–2 Transportation

It takes about 8 hours by car from the capital, Muscat, to the area, via Bidbid, Ibra, Al Kamil, etc., distance of which is about 350 km. It is provided in the all-weather highway to Al Kamil from Muscat, however, the remainder is graveled and partly rather difficult to pass. The surveyed area belongs to almost a hilly plateau, and is able to be traversed almost everywhere by 4-wheel-drive.

3–3 Topography

Generally speaking, the surveyed area belongs to the hilly plateau as a whole. In detail, however, the area is able to be divided into three pars, namely, lowland at the south of Khawr Al Jaramah Bay and Ras Al Hadd Cape, hilly land at the central part of the surveyed area and high land at the north to east of the surveyed area.

The lowland is flooded in rainy season, but drys up in dry season and allows to go by car.

Surface of the hilly plateau is gently waved and partly shows features of peneplain. The southern part of the surveyed area is gradually upheaved.

The northern to eastern part of the surveyed area has rather high elevation along the coastal line, and partly making steep slope there.

3–4 Geology

Geology of the surveyed area is involved in the geology of the Oman Mountains, because of the location of the area.

Rocks distributed in the area are the Ibra formation (Upper Permian to Lower Jurassic) and the Halfa formation (Triassic to Middle Cretaceous) belonging to the Middle Permian to Middle Cretaceous Hawasina group, and the limestone of Tertiary age (Figs. 19. 20).

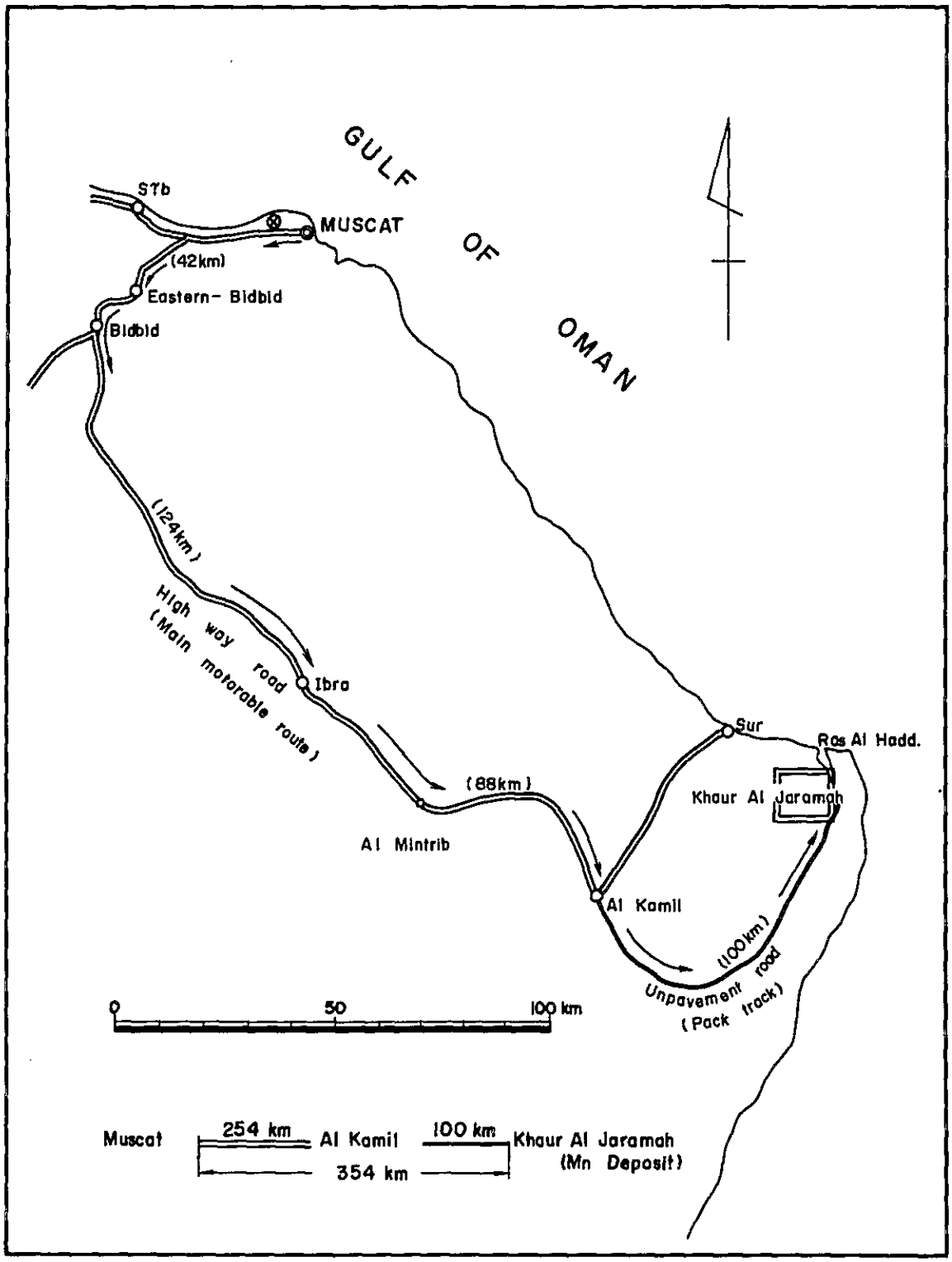

Fig. 18 Location map of the Eastern Sur area

The Hawasina group is the important strata in the Oman Mountains and investigated in detail. Name "Hawasina" was firstly used by Lees (1928), after Wadi Hawasina located in the central part of the Mountains, then subsequently used as "Hawasina group" by Kapp and Llewellyn (1965). The group is composed of sediments of oceanic floor and of turbulent flow at the marginal sea of the Arabian Plate. The group is considered to have thrust up in Late Cretaceous on the Alabian Plate together with some parts of oceanic floor of the Iranian Plate by the tectonic movements. The group is intensely suffered folding and faulting at the time of tectonic movements. The group is stratigraphically divided into many formations (about 11 formations), and the both Ibra and Halfa formations are involved individually as two formations of the group. Constituent rock facies of the group are,(1) alternations of sedimentary rocks originated from turbulent flow (such as, detritus of carbonaceous rocks, grainstone and quartz sandstone) and chert having clear bedding, (2) finegrained sedimentary rocks mainly composed of cherty materials. These layers have intensely suffered folding and faulting. The Ibra formation shows the rock facies of (1), and the Halfa formation shows that of (2).

3–4–1 Ibra Formation

The Ibra formation was named after Ibra, name of a town in the sourtheastern part of the Oman Mountains by Haramboure and Horstink (1967).

Distribution

The formation is mainly distributed forming small hills scattered on the lowland of Hollocene sediments, in the south of Khawr Al Jaramah bay and also partly in the sortheastern part of surveyed area. The thickness of the formation is not defined owing to the poor exposure in the area, however, by the assumption from the features in the type locality, it may be supposed to be less than 200m.

Lithology

Around the type locality, the formation is composed of boulder (recrystallized limestone) bearing conglomeratic layer, grainstone, shale, mudstone, sandstone and chert. In the upper part, brownish quartz sandstone increases.

In the surveyed area, the formation comprises alternated strata of brownish-dark-gray, fine- to medium-grained sandstone and gray siltstone. These alternated strata are inferred to be correlative with the brownish quartz sandstone developed in the upper part of the Ibra formation around the type locality.

Around the type locality, sandstone involves detritus of basic igneous rocks (Glennie et al, 1974). On the contrary, sandstone involves dark green glauconite scattered among quartz grains in the surveyed area. This is the characteristic feature of the sandstone developed in the surveyed area.

In the alternative parts of snadstone and siltstone, graded bedding can be frequently observed The fact shows the evidence that the snadstone is clearly turbidite. As a whole, the formation has been generated at the place where the shallow sea sediments have flown into deep sea environemnt.

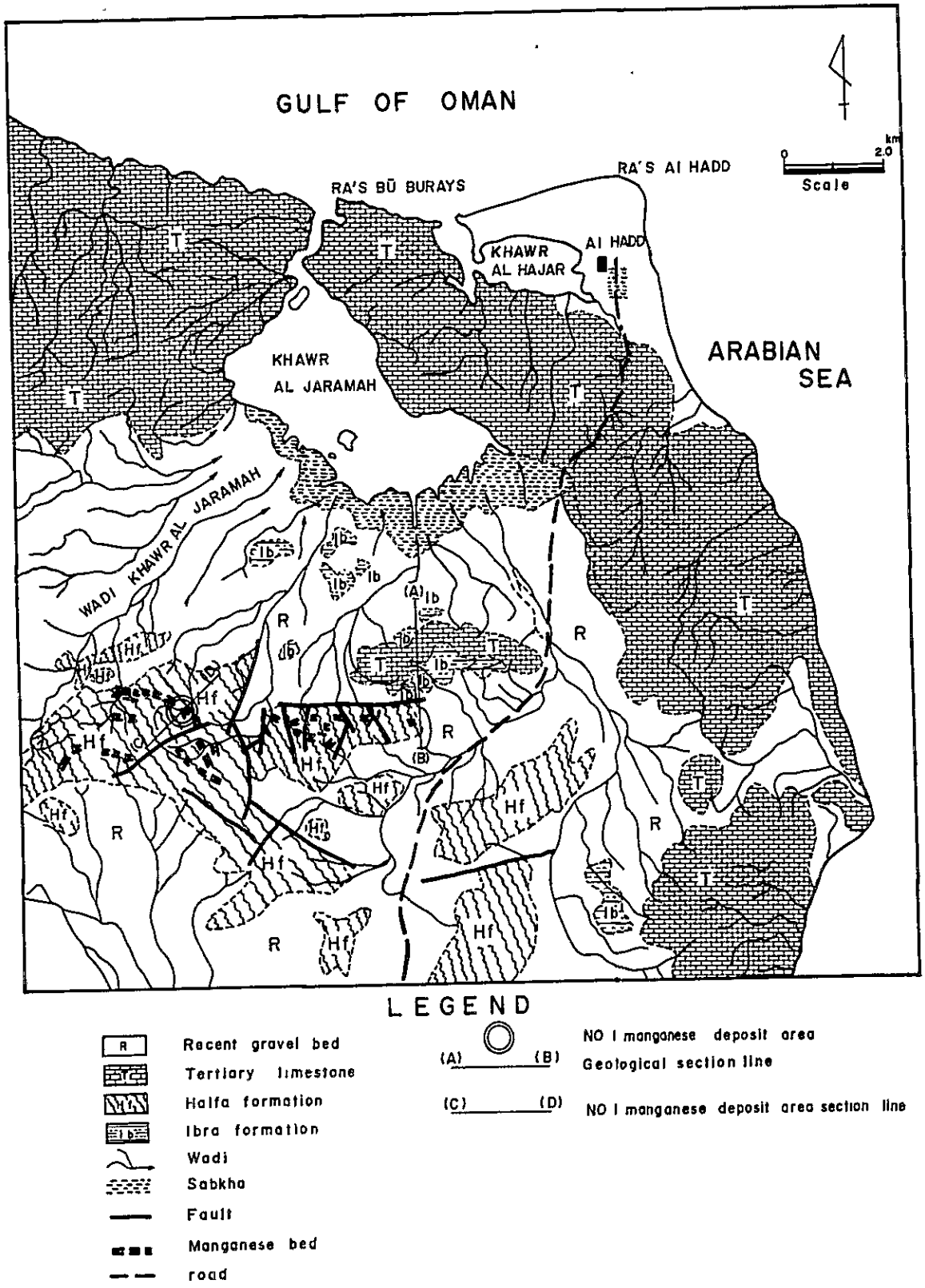

Fig. 19 Geological map of the Eastern Sur area
(by M. A. F. P. M of Oman)

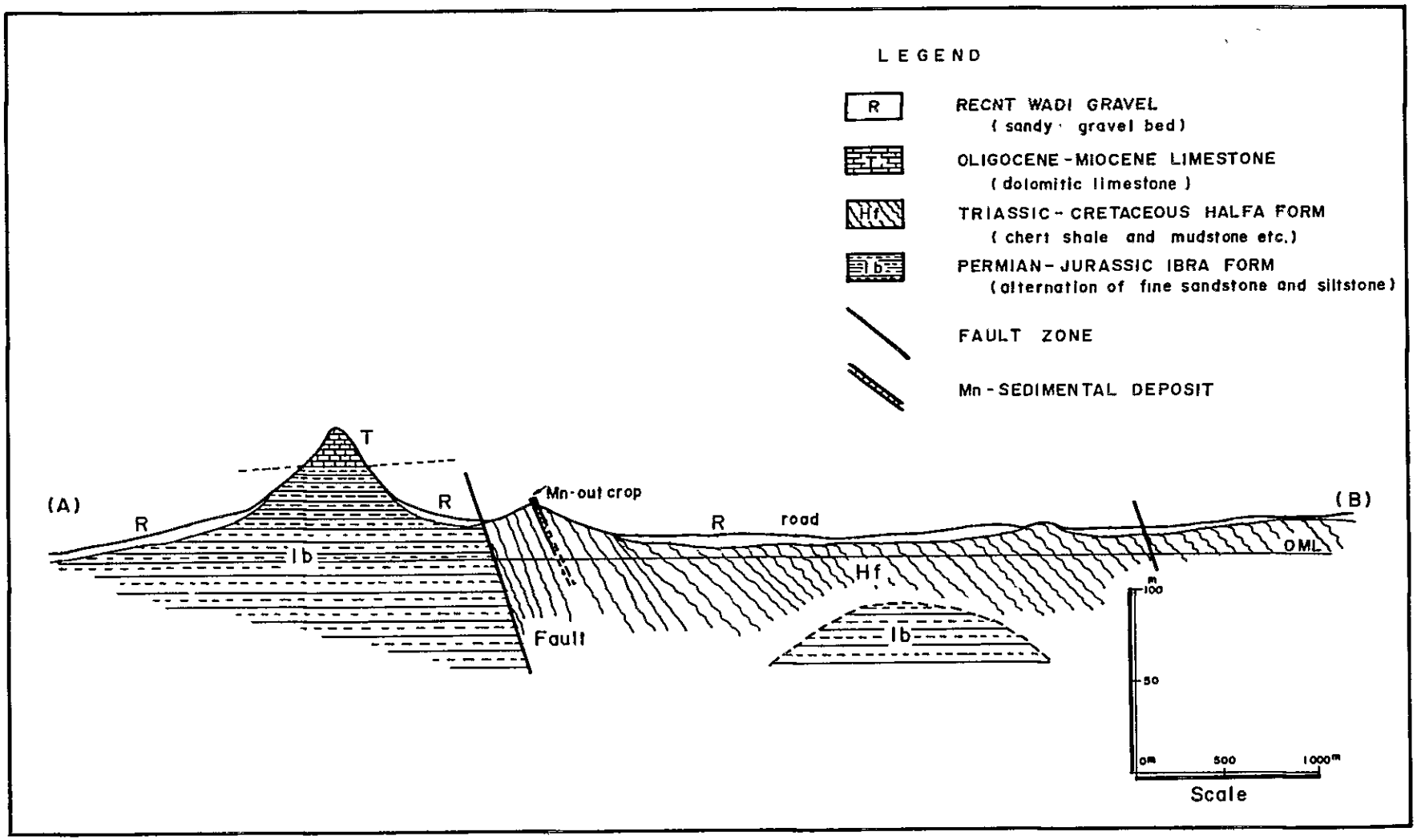

Fig. 20 Geological section of the Eastern Sur area

Age

The age of the formation is considered to be Late Permian to Early Jurrasic by the investigation of microfossils, such as, *Involutina* SPP., *Duostominidae, Mesonodosarids*, etc. (Glennie, etc., 1974).

Stratigraphical Relationship

The stratigraphical relations of the beds included in the Ibra formation are uncertain in the surveyed area because of the narrow exposures in the vertical direction. Relation to the Halfa formation is considered to be in fault contact based on the changes of strike and dip between the two formations.

Relation to the Tertiary limestone is in clear unconformity and is observable at the central part of the area.

3–4–2 Halfa Formation

The Halfa formation was named after Halfa, name of a town in the southeastern part of the Oman Mountains by Glennie etc. in 1974.

Distribution

The formation crops out widely on the hills scattered in the central and southern parts of the area.

Lithology

The formation is composed of alternations of the red~green chert including abundant radiolarians and silicious shale at the surrounding area of the type locality. In the surveyed area, rock facies are almost similar to those of type locality, but as a whole, quantity of shale or siltstone is more conspicuous.

The formation is not accompanied with shallow sea layers. Owing to this fact, it is considered that the sedimentary environment of the formation may have been abyssal on the deep ocean floor remote far from the sedimentary basin of clastic materials. Shale or silstone is pale gray to reddish brown and much of them is siliceous. Chert is intercalated as thin beds of several centimeters to ten-odd centimeters. Its color is reddish in fresh surface, but, changes to white~pale gray by weathering. Abundant radiolarians are involved in the chert. With naked eyes radiolarian can be recognized only as translucent grains, however, under the microscope, is observable as spheritic grains replaced by quartz of 0.1 ~ 0.3 mm in diameter. Surrounding parts of radiolarian are cherty and stained by red substances supposed to be iron oxide and/or muddy material.

In the surveyed area, manganese bearing chert is distributed and mineralized zones composed of manganese dioxide mineral are observed in some parts of the chert. Age of the chert is clearified to be Late Jurassic to Early Cretaceous, from the correlative study of chert distributed in the southeastern part of the Oman Mountains.

Recently, the studies on the manganese nodule and the sedimentation under abyssal environment on the ocean floor have been rapidly progressed. From the results obtained by these studies, genesis of the manganese mineralization in some chert in the Halfa formation is considered to be due to the sedimentation under the deep ocean environment, and furthermore, even the chert itself is thought to be generated from sedimentation of reddish clay on the deep ocean floor (Glennie et al., 1974).

The Halfa formation are characterized by the alternations of chert and siliceous shale and by the remarkable developments of fold and fault in the strata (Photo. 25).

Age

It is difficult to clearify the species of radiolarian in the chert, because of the complete replacement of rediolarian to siliceous substance, although abundant radiolarians are involved in the chert as mentioned above. Concerning only on the chert in the type locality, it may be possible to say that the age of deposition of the chert is in the age between Triassic to Middle Cretaceous, because *lamellibranchs (Halobia cf.)* has been identified in the chert.

Stratigraphical Relationship

As mentioned before, the formation is supposed to be in fault contact with the lower Ibra formation and to have been unconformably covered with the Tertiary limestone.

Although the thickness of the formation seems to be not so thin in appearance by its structural features such as intense folding and faulting, original thinkness is presumed to be only 130 m or so in the type locality. In the surveyed area, also, the thickness is thought to be thin, as same as that of the type locality, though intense folding may lead our misunderstanding to overlook the repeated status of the same layers.

Geological Structure

It is rather difficult to recognize general strike and dip because of the complicated features generated by the intense folding and faulting. Roughly speaking, strike in the direction of E–W seems to be predominant.

Features of the folded strata are quite complicated and different in each place. One manganese bearing horizon appeares also repeatedly in the area.

Generally speaking, fault systems in the surveyed area are observed in the directions of N–S, E–W, NW–SE and NE–SW. In addtion to these large scale faults, numerous faults in small scale cut the strata.

3–4–3 Tertiary Limestone Formation

The formation is mainly composed of shallow sea sediments of carbonaceous and marly matters of Tertiary period. It was deposited unconformably over the preexisted Hawasina group mentioned above, after the thrust movement of ocean floor complex in Late Cretaceous age. Because of the lack of fossil, it is difficult to confirm the age of the

strata in detail. Geological features of the surrounding areas make it possible to guess the age of the strata as Tertiary.

Distribution

Main distributed area of the formation is in the west to fishing port, Sur. The easternmost of the distributed area is included in the surveyed area. Namely, from the western side of the Khawr Al Jaramah Bay to the southeastern part of the surveyed area, the formation is distrubuted almost parallel to the coast line, constructing rather high plateau in 4 ~ 5-km-wide zone.

Lithology

The formation is generally composed of massive or bedded limestone and dolomitic limestone gray to dark gray in color with intercalations of thin layers of marl. Under these limy layers, basal conglomerate is developed. Gravels involved in this conglomerate are chiefly of limestone, lesser of sandstone and chert and matrix is cemented by limy sand.

Weathered surface of these rocks is mostly pale gray to pale yellow. Sometimes, the color changes to brown by the soakage of oxidized iron. Partly, limy gravels or limy matrix have been leached into ground water and left holes or durses there.

Stratigraphical Relationship

Contact to the layers below is clear unconformity accompanying basal conglomerate.

3–5 Mineral Deposits

3–5–1 Mineralized Zone

The manganese deposit in the surveyed area is interbedded in the Halfa formation and the main constituent mineral is pyrolusite.

Abundant outcrops of manganese mineralization in the surveyed area are concordantly interbedded in the cherty layers in the Halfa formation. General strike and dip of the zone are E–W (partly NW–SE) and 50^{o}~80^{o} S respectively. The zone is intermittently traceable along strike about 6 km on the ridges of hills (Photo. 26).

Average extension of each ore body is about several tens meters and its width is quite variable. Among these ore bodies, the one located at the central part of the surveyed area and extended in the direction of NW–SE, is rather large in scale, having high grade ore. This ore body is called "the first ore body" (Fig. 21).

Geological succession around the mineralized zone is quite similar in each place. Fig. 22 shows the columnar section of the geological succession of the area around "the first ore body" as a representative of the whole area.

The foot wall side of the mineralized zone in succession is composed chiefly of pale-grayish, clearly bedded, siliceous shale intercalated with thin chert. The layers change their color to light-brown by the effects of silicification and oxidation.

The lowermost part of the mineralized zone is occupied by well bedded (partly massive) chert accompanying thin layers of mudstone and is penetrated by the networked veins of quartz. The dark gray massive chert with white quartz network is quite similar to the parent rock which commonly occurs in the footwall side of bedded manganese deposits in Japan.

Mineralized zone is subdivided into three, namely, lower, major mineralized part, middle part involving manganese nodule and upper part having thin low grade ore.

The lower major mineralized part forms highest grade ore in the whole zone, and especially at the upper and lower parts, high grade ore is concentrated. The lower part is frequently penetrated by the networked veins of white quartz. The middle part intercalates cherty material and forms low grade ore, with sometimes high grade ore of vein or network.

The middle part of the mineralized zone comprises alternations of well bedded, reddish chert and siliceous shale or siltstone, containing manganese nodule bearing zone 1 ~ 2m thick. Manganese lenses up to several tens centimeters in length and small manganese nodules are also distributed in this zone.

The upper part of the mineralized zone comprises thin bands of low grade ore under 10 cm in thickness.

The hanging wall of the mineralized zone is composed chiefly of well bedded, reddish brown shale~siltstone, several to ten-odd meters in thickness, interbedding some thin bands of chert. With going up in succession, the strata change their character to grayish white siliceous shale~siltstone same as the footwall side of the mineralized zone.

Such stratigraphical succession around "the first ore body" seems to be quite similar to that around the other ore bodies. This fact is quite useful to trace the existence of the ore body even in the area having complicated structure, although in some areas complete succession is unable to be observed, owing to the existence of folds and faults.

3–5–2 Ore Minerals

Ore minerals are composed of black manganese dioxide and are determined as pyrolusite by the observation under the microscope, X–ray powder diffraction method and chemical analysis.

By the field obserbations, high grade ore including concentrated pyrolusite is rather soft but sometimes hard, having black metallic luster, and is composed of aggregation of spherical, needle like and porous crystals of pyrolusite. A part of weathered surface is ruggy because of the existence of dark gray compact manganiferous chert in the forms of network or patch. The low grade part includes a fair amount of black, compact, manganiferous chert, penetrated by the thin veins of white quartz. Under the reflected microscope, sample of the high grade ore (8–A–104) (Photomicrographs 40, 41) shows aggregations of pyrolusite. Pyrolusite is subhedral crystal of cream to white in color showing following properties: Pleochroism:

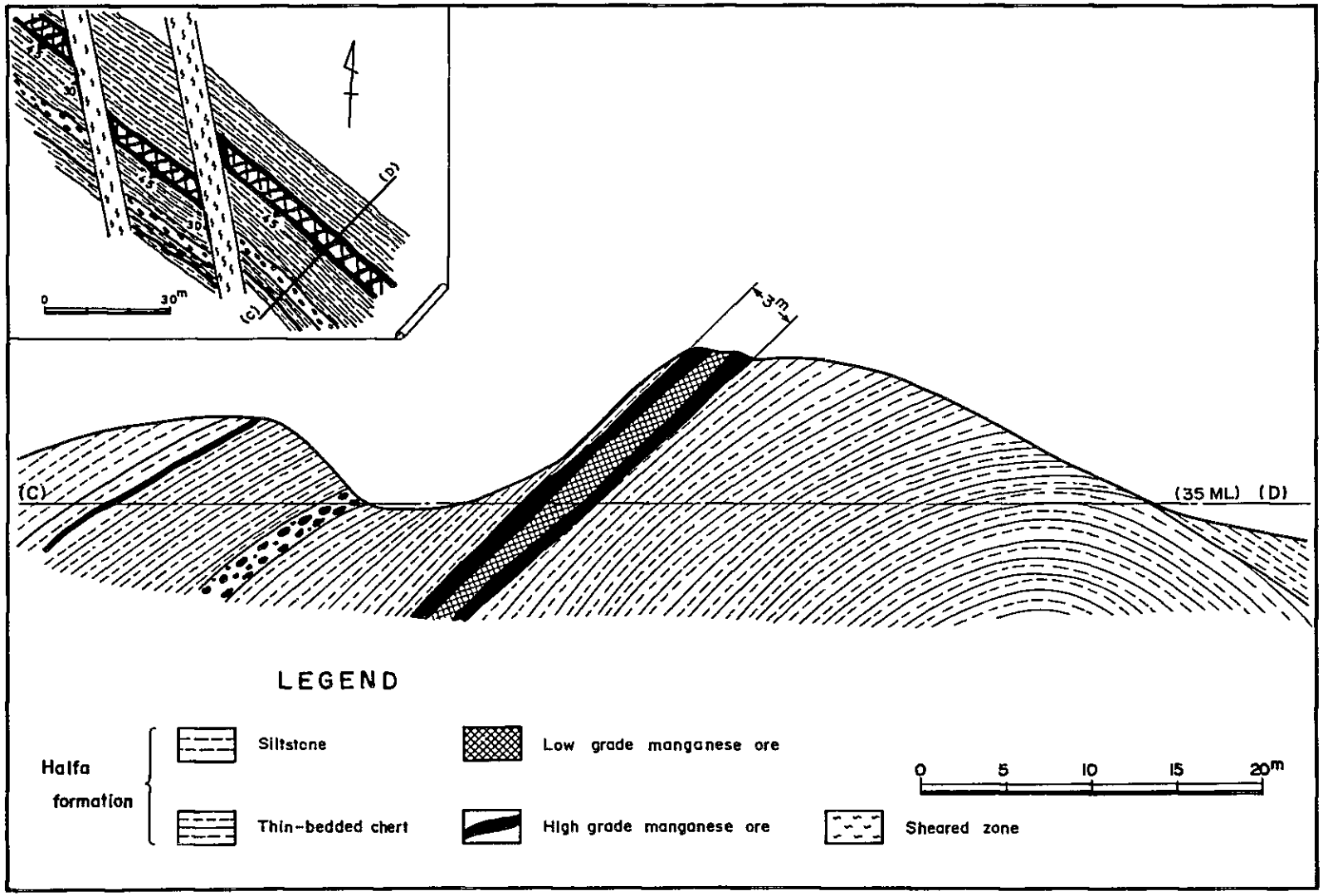

Fig. 21 Schematic geological section around the NO.1 ore deposit

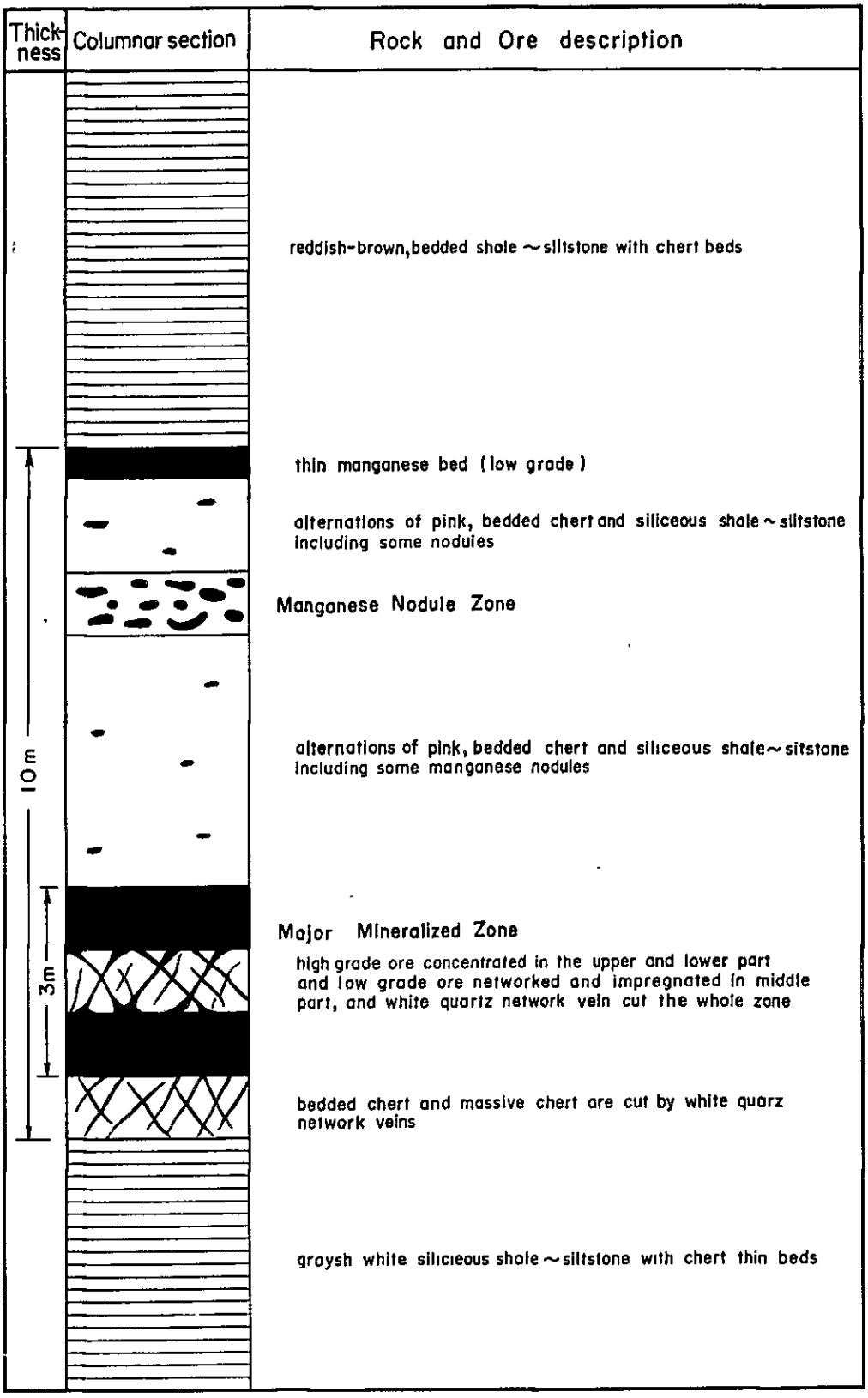

Fig. 22 Scheamatic columnar section of No.1 ore deposit area

pale yellow-dark gray isotropism: remarkably anisotropic and yellow~yellowish brown~greenish blue~gray straight extinction and twinning. These properties coincide well with those described by Ramdohr (1969).

Megascopically, sample of the low grade ore (8–A–103) is chiefly composed of black, massive, flinty, manganiferous chert. Along fissures in the chert, needle crystals of manganese dioxide (pyrolusite) are developed in the form of film. Zone of low grade ore is penetrated by the networked, thin veins of white quartz.

Under the transmitted microscope (Photomicrographs 42, 43, 44, 45), cherty materials, manganese dioxide and quartz veins cutting the ore are observable. Cherty materials are composed of fine aggregation of quartz crystals, and shows mottled texture with manganese dioxide, which interspaces quartz crystals. Abundant radiolarians are included in the chert, and the outer shells of radiolarians are replaced by quartz or manganese dioxide showing fine rings under the microscope (Photomicrographs 44, 45). Manganese dioxide is black, massive, granular or feather like, replacing cherty materials. Quartz veinlets are composed of rather coarse-grained crystals and seem to cut the chert and manganese dioxide.

The sample used for the microscopic observation, namely, 8–A–104 was again utilized for X–ray powder diffraction. As shown in Table 10 and X–ray chart 5, black minerals contained in the high grade ore show a remarkable peak of pyrolusite, coinciding clearly with the pyrolusite data in the A.S.T.M. Card. Brownish hard part of the high grade ore is mainly composed of quartz, and is accompanied by small amount of pyrolusite (d=3.11) and manganoan calcite (d=2.97) (Table 15, X–ray chart 6). Coexistence of pyrolusite and manganoan calcite observed in this part is an interest phenomenon suggesting the kind of primary minerals of the mineral deposits in the surveyed area.

The result of chemical analyses carried out on the samples collected in each ore body is shown in Table 11. High grade parts contain 53.18 ~ 54.96% Mn and 83.87 ~ 86.93% MnO_2, and low grade parts contain 28.30% Mn and 42.24~61.50% MnO_2. Also, Fe and P contents are very low. Data on the chemical analyses of the representative manganese ores in the world, namely, U.S.S.R. (sedimentary deposit), Gabon (residual deposit), Brazil (residual deposit), Australia (metamorphic deopost), India (residual and metamorphic deoposts) and Republic of South Africa (metamorphic deposit), are shown in Table 11 and in Fig. 23. Minor amount of Fe and P in the ore in this area is quite similar to those of Nikopol and Tchraturi, both sedimentary doposits in U.S.S.R..

3–6 Considerations

The manganese deposit in the surveyed area occurs in the Halfa formation of the Hawasina group. Main ore mineral of the deposit is pyrolusite. The mineralized zone is conformably distributed to the bedding plane of the host rock in one horizon of the Halfa

formation, namely, it belongs to the strata bound deposit. Lithologically, chert predominates in the horizon. Also the zone is traceable in the distance of several kilometers. These facts indicate that the deposits are primarily generated as manganese bearing chert of sedimentary origin. The chert suffered weathering and oxidation and involved manganese dioxide which has been secondarily concentrated forming higher grade than that of original ore.

Exposures of the zone are intermittently continued in the distance of about 6 km along strike side, because many faults and foldings disturb the continuity.
Individual mineralized zone can be estimated as several tens meters in strike length and several to ten meters in width in average.

The total depth of the oxidized zone is unknown, however, as the elevation of the surveyed area is about 30 m, the depth of the zone is supposed to be more than 30 m.

It is rather difficult to estimate grade of whole deposit, because number of samples taken in the present study is not so many. From the results of the chemical analyses mentioned before, followings are presumed:
Mn: 30 ~ 55%, MnO_2: 42 ~ 86%, Fe: 0.2 ~ 0.5%, SiO_2: 8 ~45%, P: 0.005 ~ 0.07%.
These results are quite similar to the data obtained from the sedimentary deposit located in U.S.S.R.

In order to confirm the distribution of the deposit, shape and continuity in detail, surface geological study based at least on the topographic map in scale 1:50,000 and the prospecting for the dip side by trenching, pitting and drilling are desirable.

It is highly possible to find out manganese deposits in the southern part to the surveyed area, because the Hawasina group is widely distributed and also the exposures of the Halfa formation are observed together with manganese gossan.

Table10 X-ray power diffraction data for black manganese mineral and brown part of No. 1 ore deposit

I			II	
2θ	d (meas.)	I	d (meas.)	I
28.7	3.11	100	3.14	100
37.4	2.40	20	2.41	50
41.1	2.20	15	2.21	10
43.0	2.10	10	2.13	25
			1.81	5
56.7	1.62	20	1.63	20
59.5	1.55	10	1.56	25

CuKα radiation
I Black ore mineral (Sample No. 8–A–104) of No.1 deposit.
II Pyrolusite A.S.T.M. 12–716

I			II	
20.8	4.27	20	4.26	35
26.6	3.35	100	3.34	100
28.7	*3.11	10		
30.1	**2.97	6		
36.5	2.46	6	2.46	12
39.4	2.29	6	2.28	12
40.2	2.24	3	2.24	6
42.4	2.13	4	2.13	9
45.7	1.99	2	1.98	16
50.1	1.82	12	1.82	17
54.9	1.67	4	1.62	7
			1.66	3
59.9	1.54	6	1.54	15

CuKα radiation

* strongest line of pyrolusite
** strongest line of manganoan calcite (A.S.T.M. 2–0714)

I Hard brown part (Sample No. 8–A–104) of No.1 deposit.
II Quartz, A.S.T.M. 5–0490

Table11 Result of chemical analyses of the manganese ores in Oman compared with other typical manganese ores in the world

Location, Sample No.		Mn %	MnO_2 %	Fe %	SiO_2 %	P	Remarks
Oman No.1 outcrop	8–A–102	53.09	83.87	0.27	8.43	0.075	11
ditto	–103	35.01	54.40	0.49	38.67	0.053	12
ditto	–104	54.96	86.93				
No.3 outcrop	–107	53.18	84.07				
No.4 outcrop	–108	39.54	61.50				
N.W. end of the ore zone	–111	28.30	42.24				
Soviet Union	Nikopol No. 1	43 ~ 45		2.5	14	0.25	1
	Tchiaturi 1st.	46 ~ 48		1.5	10	0.18	2
Gabon	Massive ore	48		5.0	4	0.15	3
Brazil	Matto Grasso	48		6.0	4	0.15	4
	Miudo	42		8.0	5	0.10	5
Australia	Grade 1	53 ~ 54		1.5	1.5 ~ 3.0	0.10	6
	Standard	47 ~ 48		7.0	9	0.13	7
India	C.P.M.O (Oriental)	48		7.5	12	0.16	8
	Nagpur	40 ~ 42		11.0	15	0.26	9
South Africa	Hotazile	48 ~ 50		14.0	6	0.05	10

Note: The ores in Oman are randomly collected. The grade of other typical manganese ores in the world means quality in the case of trade. Number in remarks is same as in Fig. 23.

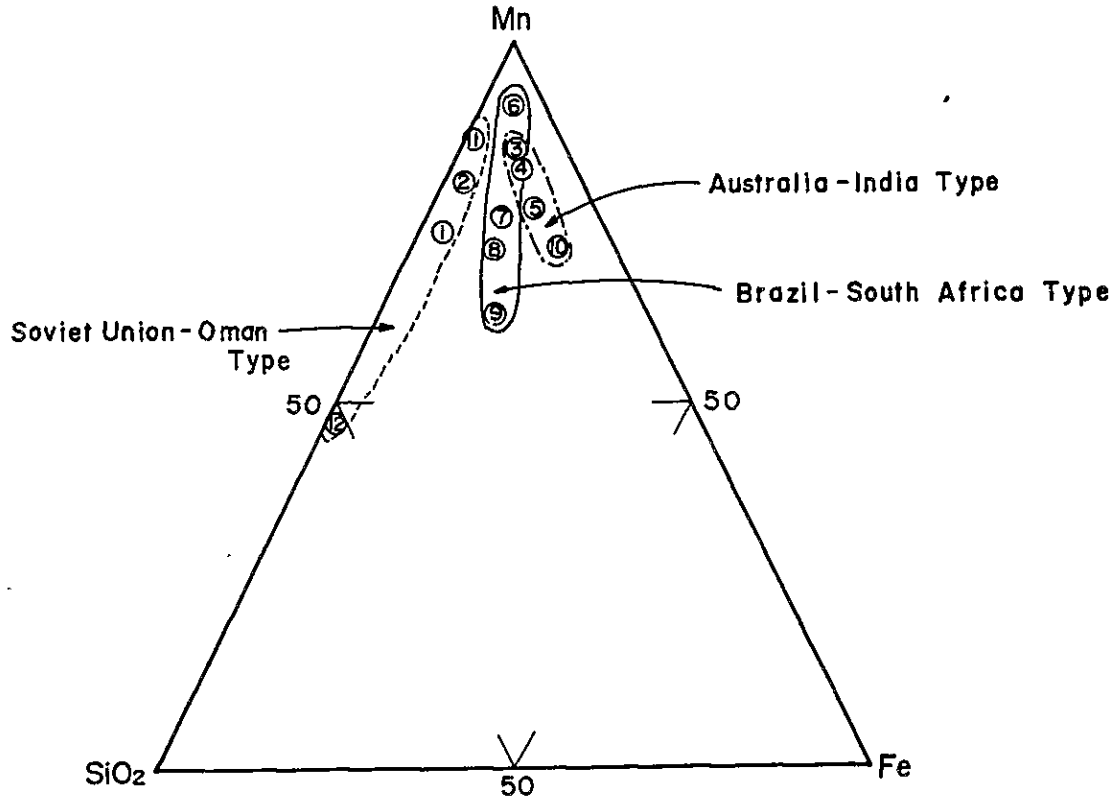

① Nikopol NO. 1 } Soviet Union
② Tchiaturi 1st }

③ Massive-ore — Gabon

④ Grosso } Brazil
⑤ Miudo }

⑥ Grade-I } Australia
⑦ Standard }

⑧ C. P. M. O (oriental) } India
⑨ Nagpur }

⑩ Hotazile — South Africa

⑪ Khawr Al. Jaramh High grade ore } Oman
⑫ High grade ore Low grade ore }

Fig. 23

Triangle diagram showing relationship of the manganese ore composition between Oman and other countries.

Photo. 25 Folding structure of the Halfa formation

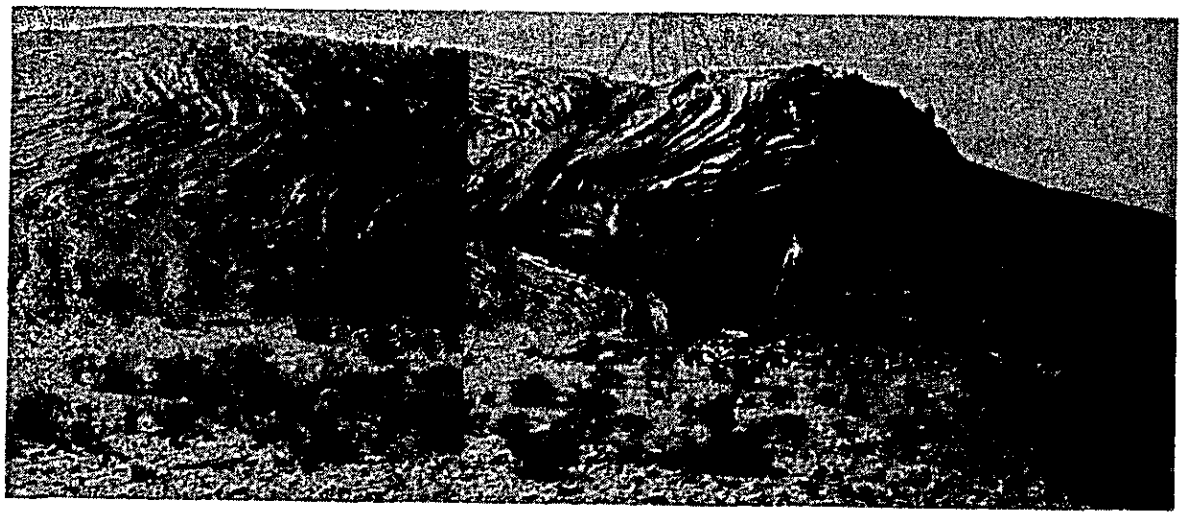

The Halfa formation composed of alternations of white chert (white part) and red siltstone (black part) shows a complex folding, and several faults are seen in the right.

Photo. 26 NW extention of No.1 ore deposit

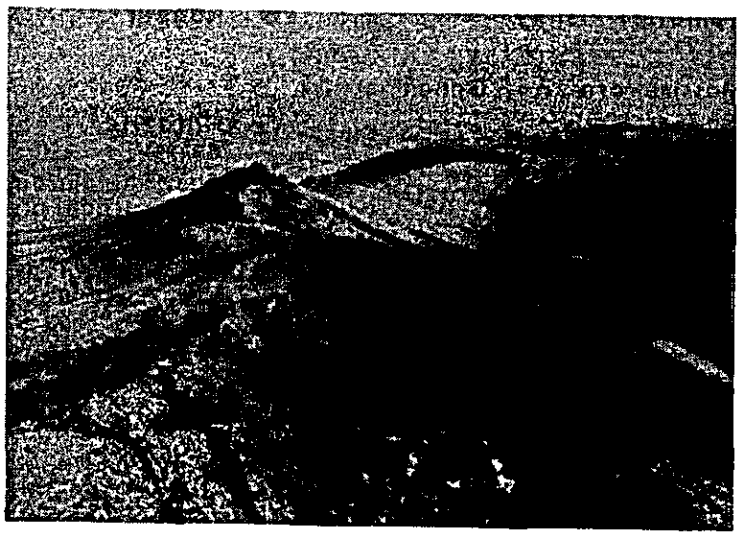

The ridges of slightly darker color compared to the slope represent a manganese ore zone which extends northwestward from the No. 1 ore deposit.

Photo. 27 Manganese ore deposit in the east to No.2 outcrop

Manganese bed shows a kink folding.

Photo 28. Manganese ore deposit close to the east end of ore zone

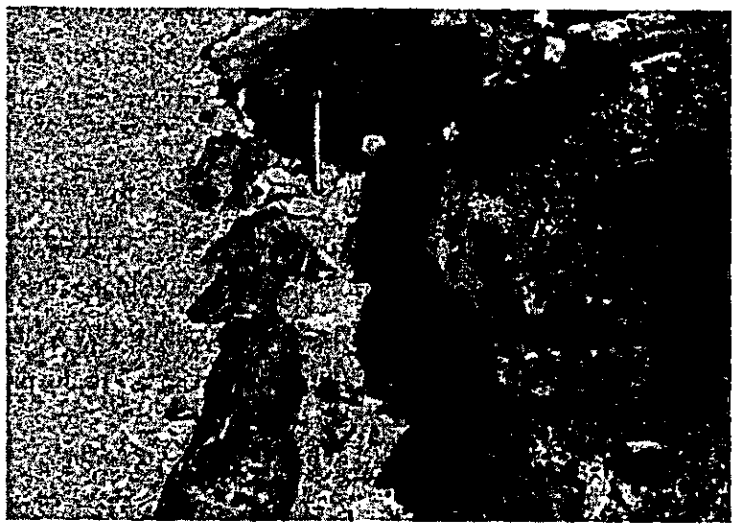

Two low grade manganese beds exist in thin-bedded chert.

Chapter 4 Batinah Coast Area

4–1 Location and Transportation

The northeastern part of Oman is constituted of fertile coastal area and the mountainous area, having Mt. Jabal Akhdar, 3,000 m in altitude. The coastal area is called Batinah plain (coast) and extends from Muscat to Sohar, a city in the north, having about 16 km in width (Fig. 24).

Mountainous area extends almost parallel to the Batinah plain, and the major part of the area is bare and barren. Even so, small part of the area has enough ground water and irrigated for agriculture since ancient time.

The paved highway between the metropolitan area and the main cities in Sohar runs parallel to the Batinah coastal line, and is only the road crowded in the country.

Present survey involves the study along the coast about 150 km in distance which corresponds to about two thirds of the total coastal line to Sohar.

4–2 Outlines of Geology and Mineral Deposit

Geology of the area is constituted of pre-Permian metamorphic rocks, Hawasina group of Upper Triassic to Niddle Cretaceous and Semail ophiolite (Fig. 24).

Metamorphic rocks at the base comprise chiefly quartzite associated with schist and phyllite sometimes amphibolite. The Hawasina group comprises limestone, sandstone, shale, siltstone and chert. The Semail ophiolite comprises pillow lava in the upper part, dolerite or gabbro in the middle and peridotite in the lower and constructs the main part of the Oman Mountains. In the peridotite involved in the Semail ophiolite, there are some chrome mineral showings. Placer chromite, the target of the present survey, is considered to have been derived from those involved in the peridotite.

Mountain range along the Batinah Coast from Muscat to the west is divided into three owing to the kinds of constituent rocks. Namely, 1) Area mainly occupied by ultra basic complex. The complex is suffered serpentinization in low grade (Sidab~Bustan area). 2) Area composed of peridotite (Seeb~Barka area). 3) Area chiefly occupied by gabbro (Musanaa~ Badaj. Ud area). Within these three areas, seven points were selected to dig pits and existence of placer cheomite were examined.

Fig. 25 illustrates the columnar sections of each pit 1m deep.

4–2–1 Sidab ~ Al · Bustan Area

At present, dredging work is in progress to enlarge the fishing port at the Sidab coast, and Al · Bustan is well known as the bathing beach to Muscatians as the sea is shallow to a long distance from the beach. Nearby the Sidab coast, sea shore is quite limited in its width, because massive peridotite,partly rather serpentinized, approaches to shore line making

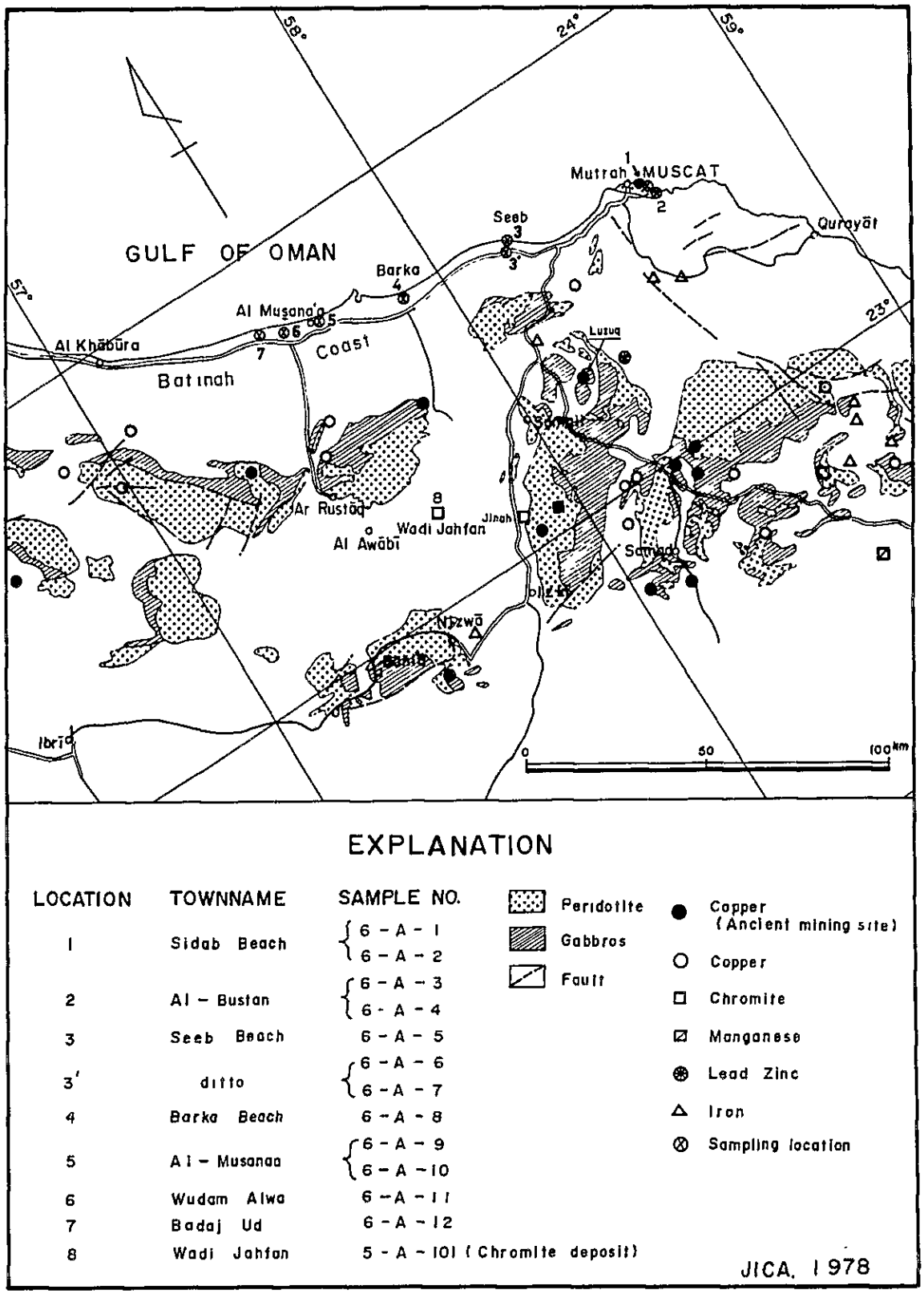

Fig. 24 Map showing the location of beach sand samples on the Batinah Coast and distribution of ophiolite.

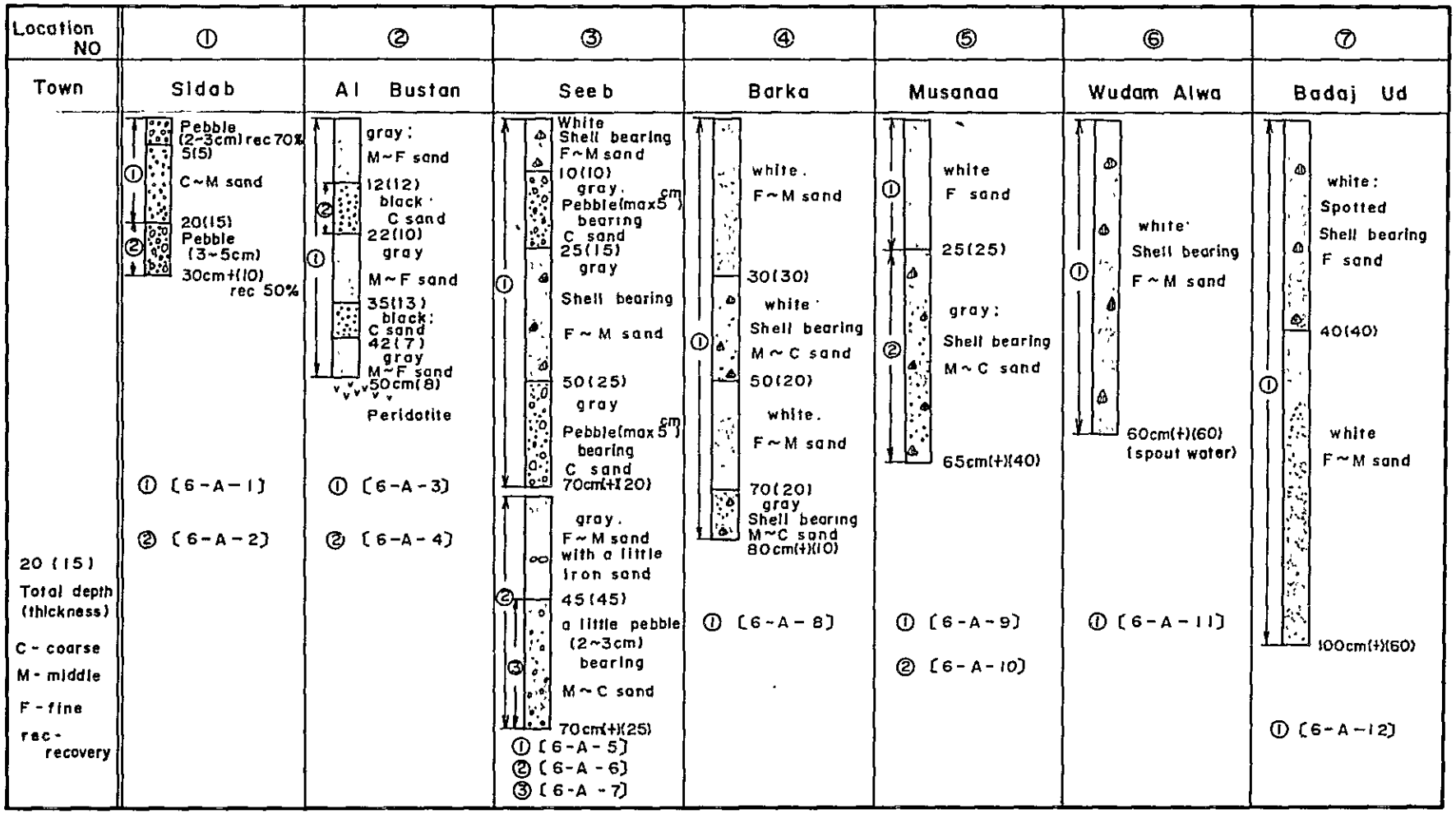

Fig. 25 Columnar section of pits for beach sand samples on Batinah Coast

cliff. At the beach near Al · Bustan, width is about 30 m and elongation is about 1.2 km or so, and exposures of basic rocks of dark green in color are scatteringly observable at the surface of beach. The present survey made a pit in the central part of the beach. By this pit it was confirmed that the beach sand is quite thin because the pit have reached at the bottom in about 50 cm to the basemental rocks of peridotite.

Grain size of beach sand in this area is chiefly coase to middle. It was clearified that the beach sand involves heavy minerals, 20 % of the total, and some iron sand by sieving analysis . using 60 mesh sieve.

Almost all of the heavy minerals are olivine, followed by diopside, chromite hornblende of light brown in color, in the quantitative ratio. Form the obtained results it was confirmed that the chromite, target mineral of the test survey, is quite small in quantity.

4–2–2 Seeb~Barka Area

International air port is located near Seeb. Area between Seeb and Barka in the west is occupied by the public institutions of various kinds, plantations, and private houses. Coastal portion of the area mentioned above has truely deep coastal sand. However, as compared with the other areas, sand here is not well sorted, and includes much of clay and gravels. In addition, sand involves fragments of shell also. Because of the reasons mentioned above, it was considered that the quantity of the heavy minerals is quite small. So the sieving analysis was omitted, although some samples were collected from sand in this coast.

4–2–3 Musanaa, Wudam · Alwa~Badaj Ud Area

The coastal area situated 60 km west of Barka is widely occupied by beach sand, except three fishing villages are located. In this coastal area, it was recognized that some black sand are scattered at the surface of the beach. Samples obtained from a pit in this coastal area were sieved by 60 mesh screen. Included heavy minerals were 50 % of the total quantity and in addition, some magnetite grains were recognized. Result of mineral identification that the most of the heavy minerals are olivine followed by diopside, sometimes aegirine augite. Important target mineral, chromite was unfortunately quite rare.

4–2–4 Chromite in Wadi Jahfan

Present survey was carried out to know the details of deposit based on the information that the exposures of the high grade primary chromite ore had been found in the Semail ophiolite distrubuted in the Oman Mountains.

1) Location and transportation

The mineral deposit is located near the bed of Wadi Jahfam about 80 km in the west to Muscat, about 270 m in altitude. It takes about 2 hours by car from Muscat to the deposit and the total distance is about 115 km.

The road from Muscat to Barka via Seeb is four-laned and completely paved, with 74 km distance, but, the road from Barka to the deposit via Afi and Nakhal farm villages is gravelled

with 40 km distance. The outcrop is characterized by black color in the surrounding brown peridotite situated in the hilly land on the bank of wadi.

2) Geology and mineral deposit

Rocks found in exposures are serpentinized peridotite. In the peridotite, chromite deposit is iron-black, lenticular, massive, compact, and shows submetallic~metallic luster. Here, chromite body shows about 9 m in width and more than 30 m in the direction of elongation. But the body is cut by the faults into three, and at the bottom (end of elongation) the body is also cut by a low angle fault. Total reserves here are estimated at about 2,000 t.

Serpentinized peridotite suffered intense serpentinization and weathering and shows brownish yellow-amber color. Peridotite below the chromite ore is partly brecciated, and even so, crystals of olivine and augite are recognized. Under the microscope, the rock shows holocrystalline structure. Constituent minerals are olivine, common augite, serpentine and chromite.

Olivine: Colorless transparent aggregates of anhedral crystals smaller than 5mm occupy about 40 % of the whole rock. It shows high refractive index and pale-yellow~pale orange pleochroism. Almost all are changed to serpentine or talc.

Common augite: Anhedral crystals smaller than 1mm showing no pleochroism and remarkable cleavage are distributed.

Chromite: Dark Brown, equigranular~semi-equigranular crystals of about 1mm in size are scattered in the matrix of olivine and common augite.

Serpentine: Colorless~pale yellow aggregates showing low refractive index cut olivine and common augite as network veins, occupying about 35% of whole rock.

Thin veins of carbonate: Thin veins of probably magnesite cut all crystals. General characters of chromite in the area will be described below. Megascopically, chromite shows black metallic luster similar to that of magnetite. It is compact and massive. Inclusions are feldspars and irregular shaped gray carbonate minerals (probably magnesite), but both are small in quantity. Under the transmitted microscope (Photomicrograph 46), chromite ore is composed of aggregates of euhedral or subhedral crystals of 2.5 mm ± in size, almost all are in aggregate form. Crystal grains are dark brown and semi-transparent, but rim and crack of individual crystal become darker or opaque owing to its increased iron content. Above mentiond inclusions are observable. Intergranular feldsper crystals cement the openings of chromite, however, all are altered and show low birefringence. Carbonate minerals, probably altered from plagioclase, are considered to be magnesite. The result of chemical analyses is shown in Table 13.

4–3 Grain Size Analysis and Checmical Analysis

4–3–1 Grain Size Analysis

Among the samples collected in the areas along the Batinah Coast, those of Al · Bustan (6–A–3) and Wudam Alwa (6–A–11) were analysed by the grain size distribution method. Obtained results are shown in Table 12. Based on the results, distribution of grain size is plotted on the logprobability paper as shown in Fig. 26, whether the grain size distribution is in normal or not.

Ninety percent of the sample 6–A–3 is occupied by sand grains, and so, the distribution curve is steep. On the other hand, sample 6–A–11 shows gentle curve in general, and this means that in case of 6–A–11, sorting is not well. Accordingly at the median value the cumulative frequency distribution is 50%, figures are $2^{-0.65} = 0.64$ mm in case of 6–A–3, and $2^{-1.75} = 0.30$ mm in case of 6–A–11. This difference is considered to have been arisen based on the difference of the processes of sorting in the two areas. Namely, in case of 6–A–3, basemental rock is peridotite and the mountains constructed of the basement crop out quite near the coast. On the other hand, in case of 6–A–11, background is the broad Batinah plain, having width of ten-odd km. Owing to these different conditions, the processes of sorting in two areas should have been also different. Again, as shown in Fig. 26, the cumulative frequency distribution curves are not in straight line. This suggests that the processes of sorting in two areas are not so simple and the sand in each area had been generated through the different process of sorting. However, portions representing normal distribution in the cumulative frequency distribution curves, are considered to indicate the sorting action generated by tidal force. Portions representing normal distribution are as follows:
In case of 6–A–3, the portion composed of coarse grains more than $2^{-1.74}$ mm in diameter occupies about 90 % of the whole. In case of 6–A–11, the portion composed of coarse grains more than $2^{-0.75}$ mm in diameter occupies about 30 % of the whole.

4–3–2 Chemical Analysis

Table 13 shows the result of the chemical analyses of chromite and other samples taken from 7 pits prepared at the Batinah Coast area. Quantity of Cr_2O_3 involved in coastal sand is 0.05 % at the Barka Area (minimum), 0.43 % at the Badaj · Ud area (maximum), and the average figure of the total 12 samples is limited to 0.155 %. Placer chromite deposit at the Batinah Coast area may be in low grade, although it is not sure because of the small number of samples. Incidentally, grade of Cr_2O_3 in the peridotite taken from Sidab coast is 0.21 %.

Grade of Cr_2O_3 in the ore collected from Wadi Jahfan area is 34 ~ 35 %, and is unsuitable for the ferro alloy industry (more than 45% is necessary) and chemical industry (more than 44 % is necessary). Content of Al_2O_3 is high (21 ~ 22 %) and it could be said that the chromite belongs to the picotite variety.

Table12 Result of grain size analyses of beach sands on Batinah Coast

Sieve Mesh	Size mm	Size 2^xmm	Sample No. 6 – A – 3			6 – A – 11		
			g	%	%*	g	%	%*
>4	>4.76	2.25	6.80	2.27	2.27	22.30	7.43	7.43
8	2.38	1.25	13.92	4.64	6.91	16.80	5.60	13.03
16	1.19	0.25	54.95	18.32	25.23	19.77	6.59	19.62
30	0.59	–0.75	81.71	27.24	52.47	21.30	7.10	26.72
50	0.30	–1.74	108.10	36.03	88.50	65.80	21.93	48.65
60	0.25	–2.00	27.90	9.30	97.80	57.09	19.03	67.68
100	0.15	–2.74	6.10	2.03	99.83	71.36	23.79	91.47
<100	<0.15	2.74	0.52	0.17	100.00	25.58	8.53	100.00
			300.00	100.00		300.00	100.00	

* cumulative %

6–A–3: Al Bustan

6–A–11: Wudam Alwa

Table 13 Result of chemical analyses of beach sand

Chemical analyses / Sample No.	Cr_2O_3%	Fe_2O_3%	FeO%	Al_2O_3%	MgO%	CaO%	SiO_2%	Cr/Fe	Location
6–A–1	0.13	–	–	–	–	–	–	–	1 Sidab
" –2	0.14	–	–	–	–	–	–	–	
" –3	0.15	2.57	–	0.95	14.00	–	11.84	–	2 Al Bustan
" –4	0.08	–	–	–	–	–	–	–	
" –5	0.18	–	–	–	–	–	–	–	3 Seeb
" –6	0.33	–	–	–	–	–	–	–	
" –7	0.07	–	–	–	–	–	–	–	
" –8	0.05	–	–	–	–	–	–	–	4 Barka
" –9	0.09	–	–	–	–	–	–	–	5 Musanaa
" –10	0.07	–	–	–	–	–	–	–	
" –11	0.14	3.36	–	1.95	14.70	–	20.24	–	6 Wudan · Alwa
" –12	0.43	–	–	–	–	–	–	–	7 Budaj · Ud
" –101 (peridotite)	0.21	–	–	–	–	–	–		7 Sidab
5–A–101 (massive ore)	34.65	16.39	0.44	21.80	14.60	0.60	1.37	2.07	8 Wadi · Jahfan

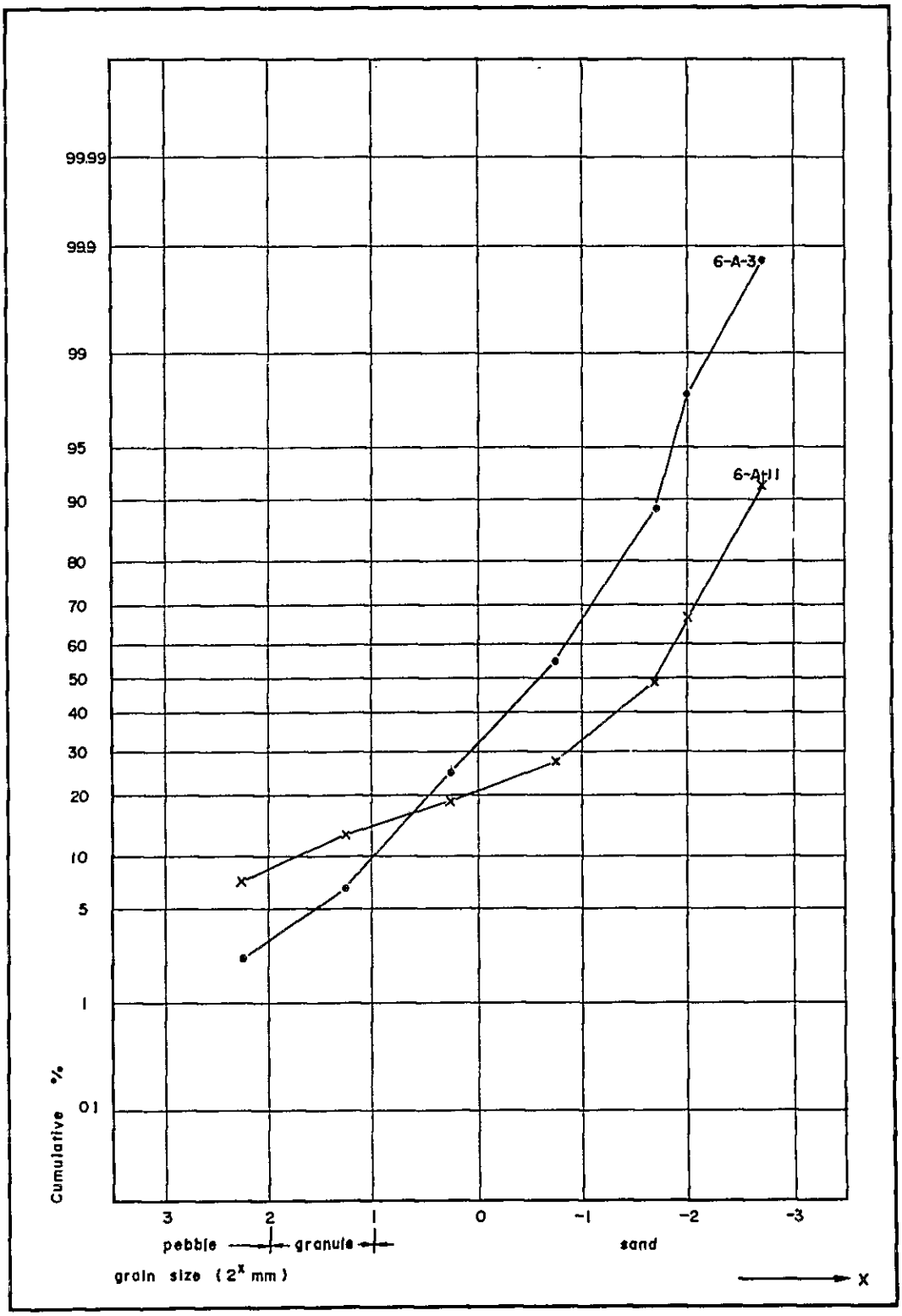

Fig. 26 Cumulative frequency distribution of grain size of beach sand on a log-probability graph, Batinah Coast

Standard of quality of chromite for the use of refractory materials in Japan is as follows:

(1) Cr_2O_3 more than 30 %

(2) $Cr_2O_3 + Al_2O_3$ more than 60 %

(3) SiO_2 less than 5 %

So, it could be concluded that the ore is not excellent for the refractory materials, because the ore fits in the conditions of (1) and (3), but does not meet for (2). Total percentage of $Cr_2O_3 + Al_2O_3$ in the ore, here, is less than 60 %.

4–4 Considerations

Test survey for the beach sand distributed along the Batinah beach, about 150 km in extension, from Muscat to NNW, has been carried out in 7 places by pit method.

Results obtained through the various analyses, it was concluded that placer chromite in the surveyed coast may not be a hopeful resources, because of the insufficiency of concentration of the ore.

Primary chromite distributed in the peridotite at the Wadi Jahfan area is insufficient in its reserves for economical use. In addition, the character of the ore is not suitable for the use of ferro alloy industry and chemical indistry, and is able to use barely for the refractory materials.

However, present survey has been carried out only for the visual exposures. So, it is too hasty to conclude the economical value of the deposits. To recognize and confirm the character and scale of the deposit of primary chromite scattered around the area, it is necessary to make study in detail.

Photo. 29 Beach sand sampling at Barka

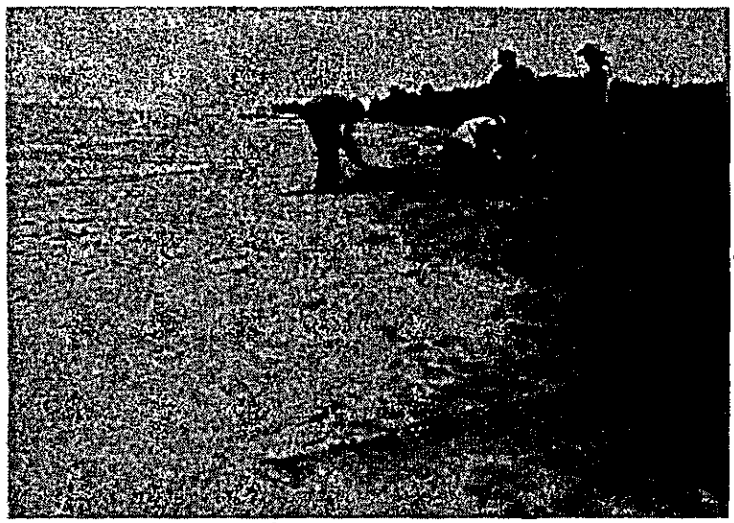

The beach at Barka develops 20 to 30 meters in width.

Photo 30 Pit for beach sand sampling

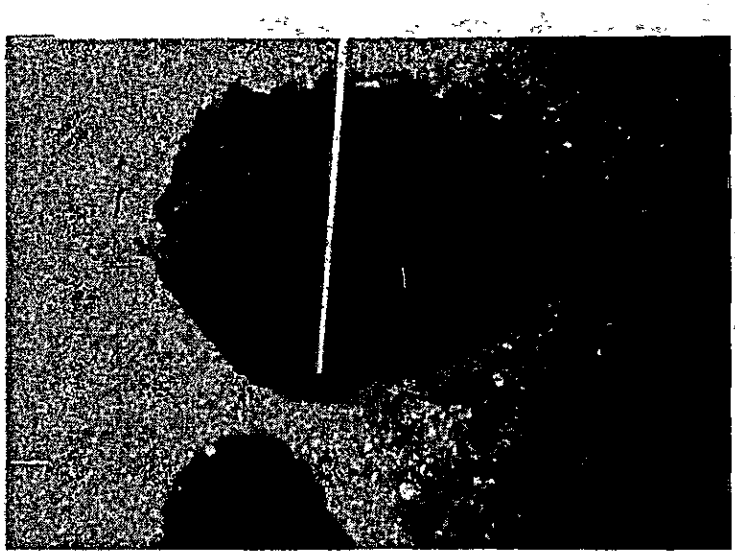

The white spots represent shells.

Photo. 31 Chrome deposit at Wadi Jahfan (5–A–101)

The chrome deposit occurs in somewhat serpentinized perioditite.

Photo. 32 Chrome deposit cut by a fault

The chromite ore body which is seen in the upper part of the top photograph is cut clearly by a gently dipping fault at its bottom.

PART III

Chapter 1 Summary

1–1 Salalah Area

1–1–1 Geology

Geology in the area consists of Precambrian basement, Ordovician Mirbat sandstone formation, Cretaceous to Tertiary Umm er Radhuma formation and Quaternary sediments.

1) Precambrian basement

It is mainly composed of Juffa gneiss (mostly garnet bearing muscovite-bioite gneiss), Sadh gneiss (mostly hornblende gneiss and quartz diorite gneiss) and igneous rocks and pegmatite~quartz vein penetrate these gneisses.

The Precambrian rocks are formed in the order of Juffa gneiss (734.7 ± 36.7 m.y.), Sadh gneiss (662.8 ± 33.1 m.y.), quartz porphyry granodiorite (640.2 ± 32.0 m.y.), pegmatite (576.7 ± 28.8 m.y.), acidic and basic dykes and adamellite stock (537.5 ± 26.9 m.y.) and these figures of age mostly represent Late Precambrian and the last figure seems to represent the end of Precambrian if a range of error is taken into consideration.

The Juffa gneiss is distrubuted in the central area showing a gentle NE–SW anticlinal structure, and the Sadh gneiss is distributed surrounding the Juffa gneiss. The igneous rocks and pegmatite intrude these gneisses, and numerous dyke swarms occur dominantly in NW–SE direction.

The igneous rocks seem to have not so remarkable differnce in age each other and to represent a series of igneous activity in the end of Precambrian. Copper, lead and other mineralizations are thought to be related to the acidic igneous activities.

2) Ordovician Mirbat sandstone formation

The formation unconformably overlies the Precambrian basement and unconformably underlies the Umm er Radhuma formation in the western area and wedges out eastward. It is tentatively correlated with the unfolded Lower Ordovician near Huqf in the Oman desert by Beydoun (1964) though fossil occurrence is not yet known.

The formation is divided into the Lower, Middle and Upper members. The grain size of clastic material constituting each member is decreased from base to top and basal conglomerate occurs on the surface of the Precambrian basement showing that it may be derived from the adjacent basement.

Sedimentary structures such as Channel structure, ripple mark and cross-bedding are observed and these structures suggest that the formation is deposited under shallow water.

The formation shows general strike of N 10°~40° E and gentle dip of NNW without remarkable faulting and folding.

3) Cretaceous~Tertiary Umm er Radhuma formation

The formation almost wholly composed of limestone unconformbly overlies the

Precambrian basement and the Mirbat sandstone formation in the upper part of escarpment, making a tableland of Jabal Samhan in the northern area. It shows nearly horizontal distribution and dips very gently to the north or east.

The formation also constitutes the top of small mountains near the coast making mesas.

4) Quaternary sediments

The raised beach sediments are distributed at 100~200 m in altitude in the central area, beach sand and aeolian sand dune near the coast, and gravel and coarse sand at the bottom of the main wadis.

1-1-2 Mineral Showings

1) Metallic minerals

Galena bearing quartz veinlet and network occur in an acidic dyke in the Juffa gneiss on the slope near the wadi where geochemical exploration was carried out at this time. A sample collected from an old pit shows 33.66 % Pb and any other metallic minerals are not observed under the microscope. The mineralized zone is thought to be discontinuous and not so large in scale because the width of the dyke is rather narrow.

Malachite associated with pyrite and limonite occurs in pegmatite in the Sadh gneiss near Wadi Khorhant, west of Sadh and a sample including malachite shows 0.32 % Cu. The mineralized zone showing impregnation and network is narrow and discontinuous.

Gossan in pegmatite and float gossan occur on Wadi Morir and Wadi Hadabin and hematite and goethite are identified by X-ray powder diffraction patterns. Also, pyrrhotite accompanied by pyrite occurs in the hanging wall side of pegmatite in the Sadh gneiss forming vein and partly small lense. All of these are of a very small scale.

The above-mentioned mineralizations have an intimate relation to acidic dyke and pegmatite though it is of vein-like shape but discontinuous and of a small scale. Of course, these seem to be of no economic value, but it is very interesting that the copper and lead mineralization had been confirmed in the Precambrian basement related to acidic dyke and pegmatite, though large scale base-metal mineralization related to acidic~intermediate volcanism as seen in Saudi Arabia seems to be unable to occur. It is necessary to carry out further survey for examining a possibility of presence of economic mineral deposits.

2) Uranium

Radioactive anomaly in the Precambrian basement has been found only on the left bank near the mouth of Wadi Ayn. A sample of muscovite-biotite-magnetite gneiss in the Sadh gneiss contains 0.003 % U_3O_8 and 0.001 % ThO_2.

On the other hand, the siltstone of the Mirbat sandstone member commonly shows nearly three times radioactivity as that of background and the result of chemical analysis on one sample shows 0.004 % U_3O_8.

This value is more than ten times as that of general siltstone.

As mentioned already, uranium deposit of large scale, such as quartz conglomerate type, anatectic type or vein type in the Precambrian Schield in the world is probably impossible to be distributed in the Salalah area owing to its geological circumstances. Concerning uranium in the Mirbat sandstone formation, there is a possibility of existence of the "sandstone type" deposit in which uranium is fixed from ground water under reducing condition. The host rock of the "sandston type" deposit generally belongs to the continental type accompanying paleochannel, intercalation of impermeable bed, carbonaceous matter, etc.. The Mirbat sandstone formation satisfies a part of such favorable conditions for uranium precipitation. If high radioactive anomaly and carbonaceous matter would be found by a further field survey, then potentiality of uranium will be increased. Therefore, it is necessary to carry out a further survey for the sedimentary structure and radioactivity in the rock.

The calcrete type, which occurs in the calcreted drainage systems of the arid and semiarid area, cannot be expected to occur in the area.

1–1–3 Geochemical Exploration

Geochemical exploration on wadi sediments, which was carried out to examine the applicability of wadi sediments and also to examine the most favorable location across the wadi bed, does not show any excellent results. Metal contents are very low and less variable though only one location 200 m to the old lead pit shows an effect of lead mineralization by lead content of 20 ppm. Form the result of this geochemical exploration together with the previous result of Taylor Woodrow-Towell Co., geochemical exploration is thought to be not effective as a regional exploration method in the Salalah area.

1–2 Eastern Sur Area

1–2–1 Geology

The area is composed of the Ibra formation of Upper Permian to Lower Jurassic and the Halfa formation of Triassic to Middle Cretaceous belonging to the Hawasina group and Tertiary limestone.

The Hawasina group is thought to have been originally sedimented on the Arabian Plate and thrusted up together with the Semail ophiolite of the Iranian Plate in Middle Maestrichtian owing to the collision between the both Plates. It is composed of turbidite, pelagic sediments, etc. and shows remarkable faulting and folding structures.

1) Ibar formation

The Ibra formation is composed of alternations of brown to dark gray, fine- to medium-grained sandstone and gray siltstone, and the sandstone is characterized by dark green glauconite inclusions and is thought to be turbidite with abundant graded bedding.

It is distrubuted in a narrow area south of Khwr Al Jaramah, and is inferred to have a fault relation to the Halfa formation.

2) Halfa formation

The Halfa formation is composed of red, green or white chert and siliceous shale or siltstone and is characterized by remarkable folding and faulting as well as clear-bedding. It is thought to be pelagic and abyssal and includes abundant radiolarians in chert. The manganese occurs in the central part of the area associated with chert.

3) Tertiary formation

The Tertiary formation is composed of gray to dark gray, bedded or massive limestone~dolomitic limestone with thin intercalations of marl. It unconformably overlies the above-mentioned formation in the northeastern to eastern area distributed parallel to the coast line.

1–2–2 Mineral Deposits

The manganese deposit occurs in chert zone of the Halfa formation owing to the concentration of black manganese dioxide by weathering. Ore mineral is pyrolusite (β-MnO_2). Many manganese outcrops are distributed in the area and their general strike is E–W. The mineralization zone is intermittently traceable along its strike about 6 km though folded and faulted.

As the result of chemical analyses of collected samples from the outcrop, high grade part shows 53.09~54.96 % Mn and 83.87~84.07 % MnO_2 and on the other hand, low grade part shows 28.30~35.01 % Mn and 42.24~54.40 % MnO_2, and the both parts contain little Fe and P. The high grade part is avilable for raw material of ferro alloy and buffer in dry battery.

The Hawasina group is widely distributed in the south to the surveyed area and some exposures of the Halfa formation are accompanied with gossan.

1–3 Batinah Coast

The result of test for sand chrome by about one meter deep pits shows very low concentration of heavy minerals and it is thought that possibility of high concentration of chromite is hopeless. Also, the exposure of chromite deposit in peridotite at Wadi Jahfan is blocked in by faults and the strike and dip extentions seem to be small. Also, its chemical composition shows higher Al_2O_3 and lower Cr_2O_3 and is thought to be available for refractories. It is difficult to select the Batinah Coast as a hopeful area of mineral resources.

Chapter 2 Conclusions

As the result of the comprehensive field and laboratory investigations on the geology and mineral deposit in the three areas which were offered by the Government of Oman, the Salalah area and the Eastern area of Sur are thought to be worthwhile to carry out survey further in more detail.

2–1 Salalah Area

A fundamental survey should be carried out to examine the possibility of occurrence of mineral deposits because some mineral showings of copper, lead, etc., related to pegmatite and acidic dyke in the Precambrian basement and uranium in the Mirbat sandstone have been confirmed. Therefore, following surveys are of major importance.

1) Survey to confirm the mineralization around the acidic igneous rocks such as acidic dyke, stock and batholith.

2) Survey to make clear the distribution, sedimentary structure and radioactivity of the Mirbat sandstone formation.

In the above-mentioned survey, it is desirable to make the topographic map in scale of 1:50,000 and to carry out more detailed photogeological interpretation followed by ground check.

2–2 Eastern Sur Area

A further survey should be carried out also in this area, because manganese mineralization of high grade and the extensive distribution of the Hawasina group comprising partly manganese gossan in the Halfa formation have been confirmed. Therefore, the following surveys are of major importance.

1) Regional geological survey

Investigation on the possibility of regional existence of manganese deposits by clarifying the distribution and geological structure of the Halfa formation by means of topographic map in scale of 1:50,000 and photogeological interpretation together with field survey.

2) Evaluation of the manganese outcrops already known

Clarifying lower continuity of oxidized zone and variation of grade both on strike and dip sides by detailed geological survey of the outcrop and its adjacent area together with trenching and pitting followed by drilling.

References

Beydoun, Z. R., 1966, Geology of the Arabian Peninsula – Eastern Aden Protectorate and part of Dhufar. U. S. Geol. Surv. Prof. Paper, 560–H, P. H1–49.

1970, Southern Arabia and northern Somalia: comperative geology. Phil. Trans. Roy. Soc. Lond. A. 267, p 267–292.

Brown, G. F. and Jackson, R. O., 1960, The Arabian Shield: Internat. Geol. Cong., 21st, Copenhagen 1960, Rept. 21, Pt. 9, p. 69–77.

Carney, J. N. and Welland, M. J. P., 1974, Geology and mineral resources of the Oman Mountains. Institute Geol. Soc. London Rept. No. 27, p. 1–49.

Daly, R. A., 1933, Igneous rocks and the depth of the earth. p. 9–10, Mcgraw-Hill Book Company, Inc., New York.

Delfour, J., 1975, Volcanism and mineral deposits of the Arabian-Nubian Shield. p. 1–36. Ministry of Petroleum and Mineral Resources, Saudi Arabia B. R. G. M. Saudi Arabia Mission.

Gealey, W. K., 1977, Ophiolite obduction and geologic evolution of the Oman Mountains and adjacent areas. Geol. Soc. America Bull., v.88, p.1183–1191.

Geukens, F., 1966, Geology of Arabian Peninsula – Yemen. U. S. Geol. Surv. Prof. Paper, 560–B, p. B1–23.

Glennie, K. W. and others, 1974, Geology of the Oman Mountains, Pt. 1 (Text) and Pt. II (Tables and Illustrations). Verh. Konink. Nederlands Geolo. Mijnbowkundig Genootschap, Deel 31, p. 1–423.

Greenwood, J. E. G. M. and Loney, P. E., 1968, Geology and mineral resources of the Trucial Oman Range. Inst. Geol. Sci. London, Unpublished report, p. 1–108.

Heremboure, J. and Horstink, J., 1967, Mesozoic nappes in the Oman Mountains, a hypothesis. Unpublished PD (Oman) Report.

Ishihara, S. and others, 1967, Uranium content of Upper Paleozoic slate and Neogene siltstone. Rept. Geol. Surv. Japan, No. 232, p. 221–231. (in Japanese with English abstract).

Kapp, H. and Llewellyn, P. G., 1965, The geology of the Central Oman Mountains. Unpublished PD (Oman) Report.

Katada, M., 1967, Ryoke metamorphic belt in the northern Kiso district, Nagano prefecture. Rept. Geol. Surv. Japan, No. 223, p 1–38. (in Japanese with English abstract)

Lees, G. M., 1928, The geology and tectonics of Oman and of parts of southeastern Arabia. Quart. Jour. Geol. Soc. London, v. 84, p. 585–670.

Perters, Tj. and Kramers, J. D., 1974, Chromite deposits in the ophiolite complex of Northern Oman. Minel. Deposita, v. 9, p. 253–259.

Powers, R. M. and others, 1966, Geology of the Arabian Peninsula – Sedimentary geology of Saudi Arabia. U. S. Geol. Surv. Prof. Paper, 569–D, p. D1–147.

Roberts, R. J. and others, 1975, Mineral deposits in western Saudi Arabia. U. S. Geol. Surv. Saudi Arabian Project Report 201, p. 1–60.

Saudi Arabia Directorate General of Mineral Resources, 1976, Mineral resources activity 1390–1395 A. H. (1970–1975 A. D.). A report of the first Saudi Arabia Five–Year Development Plan.

Shibata, H., 1968, Description on the rocks of Japan, II, p. 152. Asakura Shoten, Tokyo. (in Japanese)

————, 1968, ditto, IV, p. 128. ditto.

Welland, M. J. P. and Mitchell, A. H. G., 1977, Emplacement of the Oman ophiolite: A mechanism related to subduction and collision. Geol. Soc. America Bull., v. 88, p. 1081–1088.

ANNEX

Table3 List of result of microscopic observation (thin section)

Area	Group	Sample No.	Rock name	q	pl	kf	bio	mus	hb	py	ol	ga	mt	chr	ap	sph	ser	chl	sep	ep	zoi	ca	Remarks
Salalah	Juffa gneiss	22-3-2	bio gneiss	○	◎		◎						●		●	●							holocrystalline, gneissose texture, & dioritic
		25-1-1	ga bearing mus bio gneiss	◎	◎		○	○				●	●		●		●						ditto ditto
		25-2	ditto	◎	◎		◎	○				●	●		●			●					ditto ditto
	Sadh gneiss	22-8	mus mt injection gneiss	◎	○	◎	●	●					○		●	●						●	ditto , granitic, ca veinlets
		27-A-103	gneissose bio q diorite	◎	◎	●	○						●			●	●	●		●			ditto ,coarse grained, almost all bio is a altered to ep and chl
		28-A-101	gneissose bio hb q diorite	○	◎		●		◎				●		●	●	●	●		●	●		ditto , equigranular, felsic part
		28-A-102	hb gneiss		◎				◎				●			●	○			●	●		ditto , mafic part, gabbroic
		28-A-103	hb gneiss	○	◎				◎				●		●	●	○	●		●	●		ditto , equigranular, felsic part, q dioritic
		28-A-104	gneissose hb q diorite	○	◎				◎				●			●	●	●		○	○		ditto , felsic part, little goethite is present
		28-A-109	hb gneiss	○	○				◎				●		●	●	●			●			ditto , mafic part, q gabbroic
		28-A-110	hb gneiss	○	◎				◎				●		●	●	○		●				ditto , felsic part, q dioritic
		28-A-111	gneissose hb gabbro		◎				◎				●		●	●	○	●		●	●		ditto , equigranular,
	quartz diorite granodiorite	22-3-1	mus bio q diorite	◎	◎	●	○	●					●		●	●	●	●		●			holocrystalline, medium-grained
		22-5-1	trondjemite	◎	◎		●						●					●		●			ditto dyke in 22-5-2, coarse-grained
		22-5-2	bio hb diorite	○	◎		○		○				●		●	●	●				●		ditto
		22-6	mus bio granodiorite	◎	◎	◎	●	●					●			●	●	●		●		●	ditto , equigranular , carbonate vein
		27-A-101	hornblendite		○			○	◎								●			●	●		ditto , porphyritic xenolith in granodiorite
		29-A-102	mus q diorite	◎	◎			●								●	●					●	ditto , calcite veinlets
	pg	27-A-105	mus pl q perthite pg	◎	◎	◎		●									●						ditto , Kf shows perthite structure
	dyke basic	25-1-2	py dolerite	●	◎				·	◎			○				●	●				●	ditto , intergranular texture, q is secondary, strongly altered
		26-A-103	bio py q dolerite	○	◎		○			○			●				●	●				●	ditto ditto , whole py phenocryst is altered to ch and ca
		26-B-102	bio py dolerite		◎		○			◎			●				●					●	ditto ditto , some bio is atered from py, mont is present
	dyke acidic	22-2	hb adamellite	◎	◎	◎			●				●		●	●	●	●					ditto , equigranular
		25-3-1	q porphyry	○	●			●									◎						ditto , porphyritic, almost whole feldspar is altered to sericite
		25-3-2	mus bearing granophyre	◎	◎			●									●			●		●	ditto ditto , myrmekite ~ granophyre structure is well developed
		26-B-101	q porphyry	◎	◎			○		●							○					●	ditto ditto , strongly sericitized
	Umm	22-3-3	sandstone	◎																			matrix is composed of fine-grained silicate and spheruritic goethite
	Mirbat Sandstone	22-9	siltstone	◎				●															bedding structure
		22-10	arkose sandstone	◎	◎	○	○	●														○	very coarse, matric is composed of carbonate
		29-A-101	sandstone (matrix of congl)	●	●			●														◎	granitic rock granules are abundant, matrix is composed of carbonate
		29-A-103	sandstone	◎	●			●									○					●	coarse, matrix is composed of ser. kaoline, limonite and ca
Eastern Sur	Hafa formation	8-A-101	massive chert	◎																			pyrolusite and radiolaria are rare, unknown black material exists
		8-A-103	low grade ore	◎																			pyrolusite is abundant, radiolaria is rare
		8-A-112	radiolaria chert	◎																			radiolaria is abundant, dust like tiny brownish red mineral is abundant
Batinah Coast	ophiolite	5-A-101	chromite ore		●									◎								●	holocrystalline
		5-A-102	py bearing peridotite							○	○			●					◎				ditto , strongly serpentinized
		6-A-101	ol bearing pyroxinite							◎	○			●					◎				ditto
	beach sand	6-A-3	beach sand	●						○												◎	peridotite fragment is present about 20%, carbonate represents shells
		6-A-3	beach sand (heavy part)						●	◎	○			◎								●	hyperthene is present about 5%
		6-A-11	beach sand	●					●	○									○			◎	sep occurs as rock fragments, carbonate represents shells
		6-A-11	beach sand (heavy part)						●	◎	○			○								●	

Abbreviations

pg : pegmatite Umm : Umm er Radhuma formation q : quartz pl : plagioclase kf : potash feldspar bio : biotite mus : muscovite hb : hornblende py . augite ol : olivine ga : garnet mt : magnetite chr : chromite ap : apatite sph : sphene ser : sericite chl : chlorite sep : serpentine ep : epidote zoi : zoicite ca : carbonate mont : montmorillonite

◎ abundant ○ common ● rare

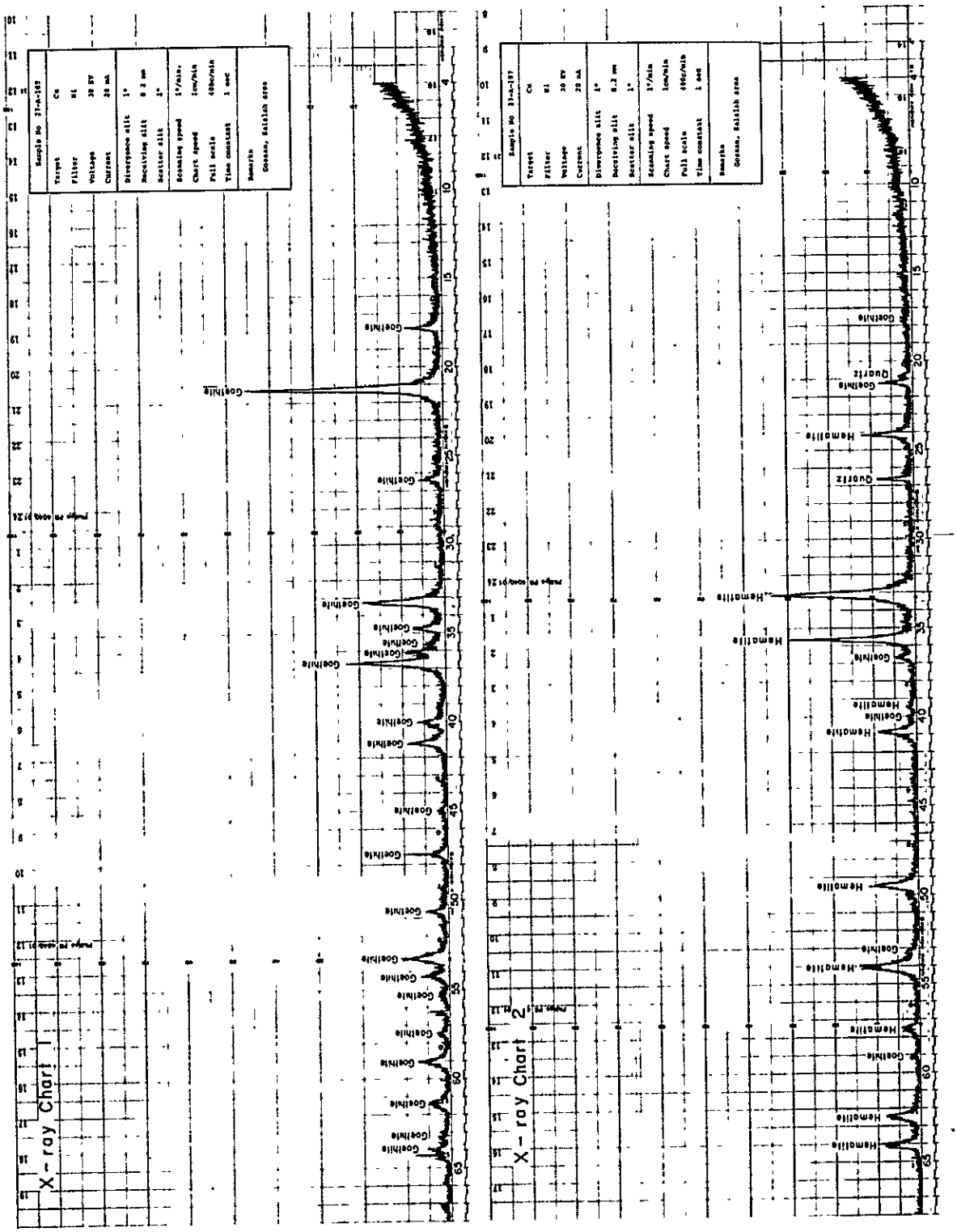
X-ray Chart 1
X-ray Chart 2
Goethite
Hematite
Quartz

X-ray Chart 3
Sample No. 25-6-196
Target Cu
Filter Ni
Voltage 30 KV
Current 20 mA
Divergence slit 1°
Receiving slit 0.2 mm
Scatter slit 1°
Scanning speed 1°/min
Chart speed 1cm/min
Full scale 400c/min
Time constant 1 sec
Remarks
Green mineral in pegmatite, Satsuki area
Chlorite
Sericite
Plagioclase
Calcite
Malachite
K-Feldspar
Quartz
Azurite?
Chlorite, Calcite
Hematite?
Quartz + Chlorite
Calcite, Quartz
X-ray Chart 4
Sample No. 25-9
Target Cu
Filter Ni
Voltage 30 KV
Current 20 mA
Divergence slit 1°
Receiving slit 0.2 mm
Scatter slit 1°
Scanning speed 1°/min
Chart speed 1cm/min.
Full scale 400c/min
Time constant 1 sec
Remarks
Kaolinite
Sericite
Quartz

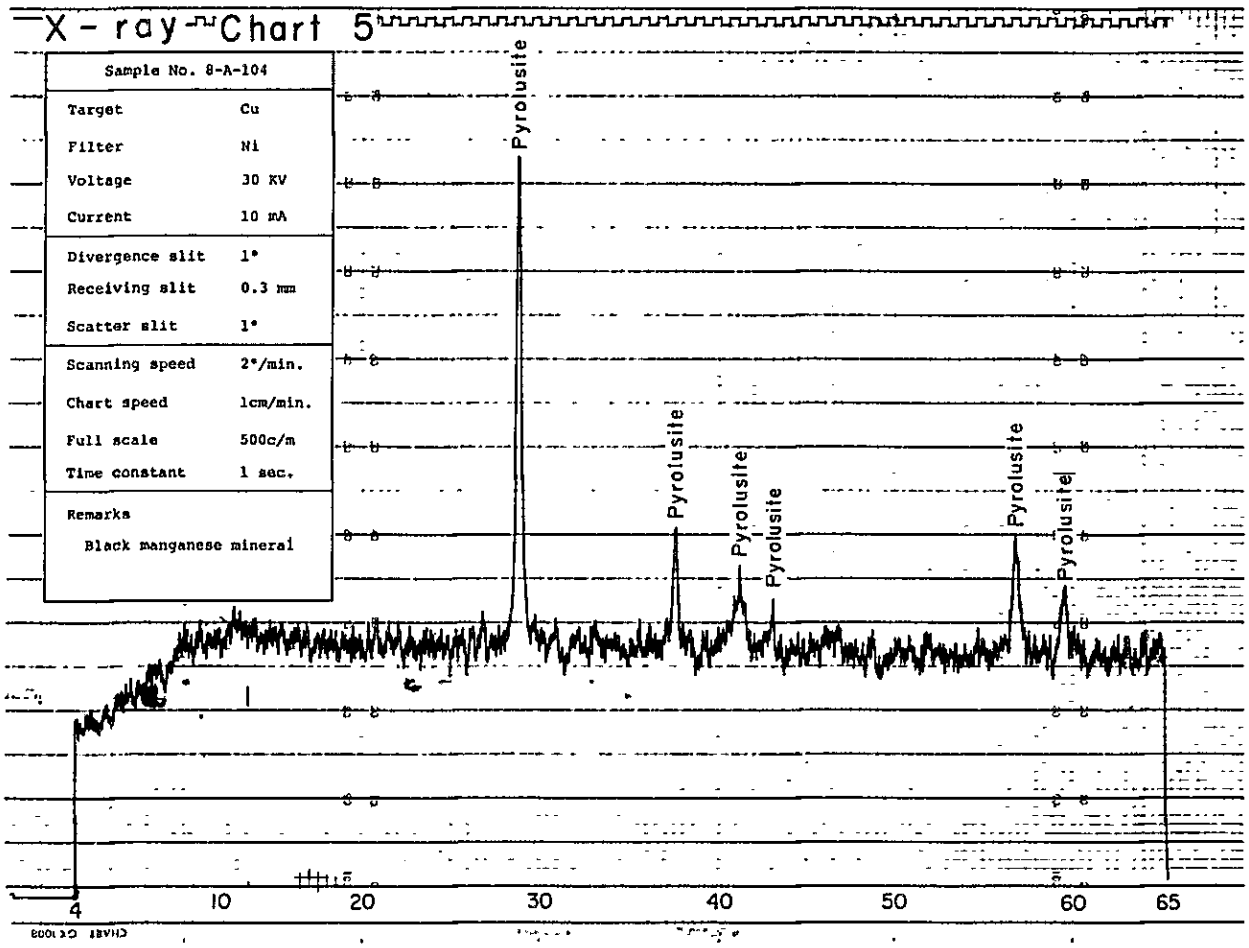
X - ray Chart 5
Sample No. 8-A-104
Target Cu
Filter Ni
Voltage 30 KV
Current 10 mA
Divergence slit 1°
Receiving slit 0.3 mm
Scatter slit 1°
Scanning speed 2°/min.
Chart speed 1cm/min.
Full scale 500c/m
Time constant 1 sec.
Remarks
Black manganese mineral
Pyrolusite
Pyrolusite
Pyrolusite
Pyrolusite
Pyrolusite
Pyrolusite
4
10
20
30
40
50
60
65

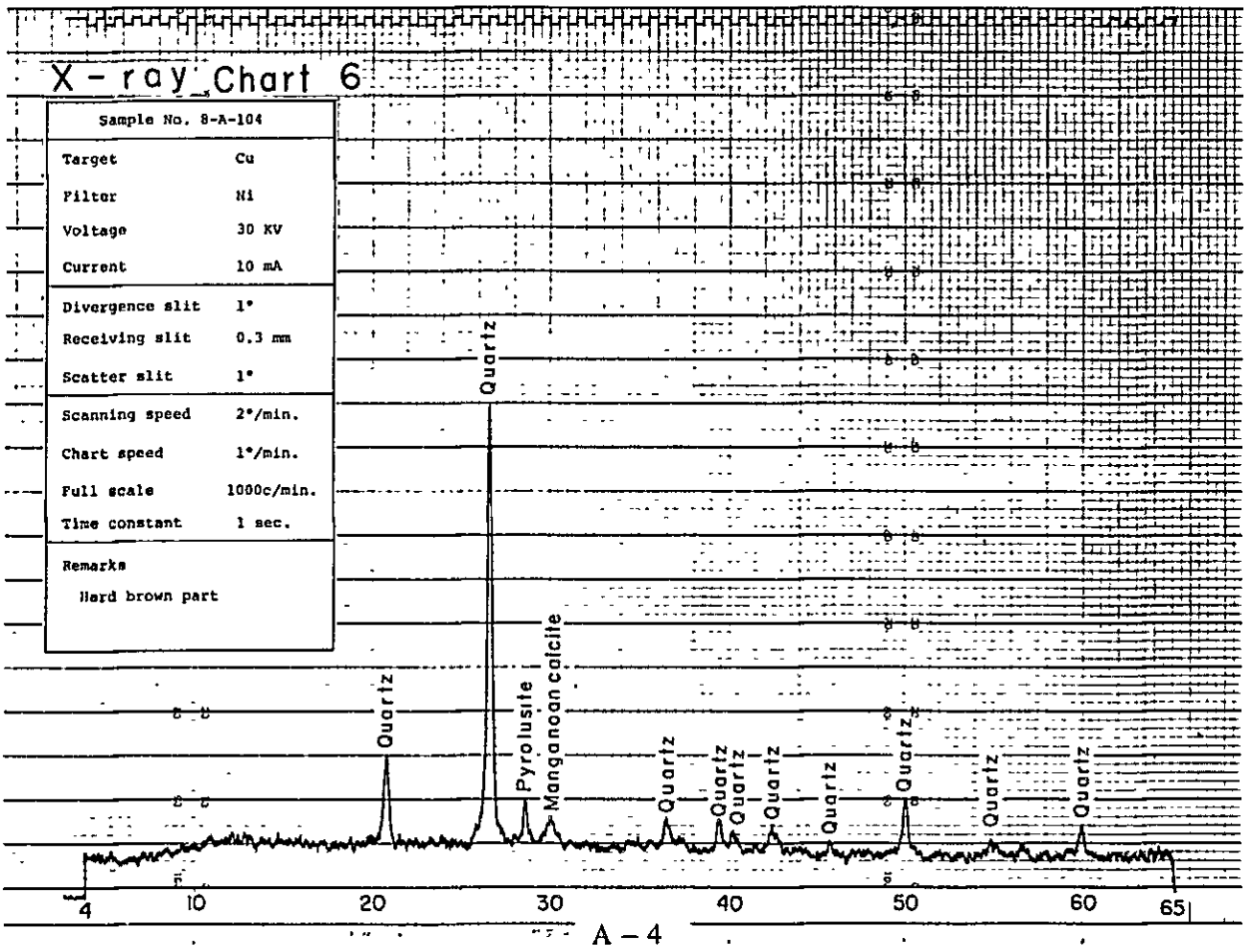
X - ray Chart 6
Sample No. 8-A-104
Target Cu
Filter Ni
Voltage 30 KV
Current 10 mA
Divergence slit 1°
Receiving slit 0.3 mm
Scatter slit 1°
Scanning speed 2°/min.
Chart speed 1°/min.
Full scale 1000c/min.
Time constant 1 sec.
Remarks
Hard brown part
Quartz
Quartz
Pyrolusite
Manganoan calcite
Quartz
Quartz
Quartz
Quartz
Quartz
Quartz
Quartz
4
10
20
30
40
50
60
65

Photomicrographs

Abbriviations

q	quatz
pl	plagioclase
kf	potash feldspar
bio	biotite
mus	muscovite
hb	hornblende
py	augite
ol	olivine
ga	garnet
mt	magnetite
chr	chromite
sph	sphene
ap	apatite
ser	sericite
chl	chlorite
sep	serpentine
ep	epidote
zoi	zoicite
ca	carbonate
gal	galena
pyr	pyrolusite
rad	radiolarian

Photo micrograph 1

Only lower polar

Photo micrograph 2

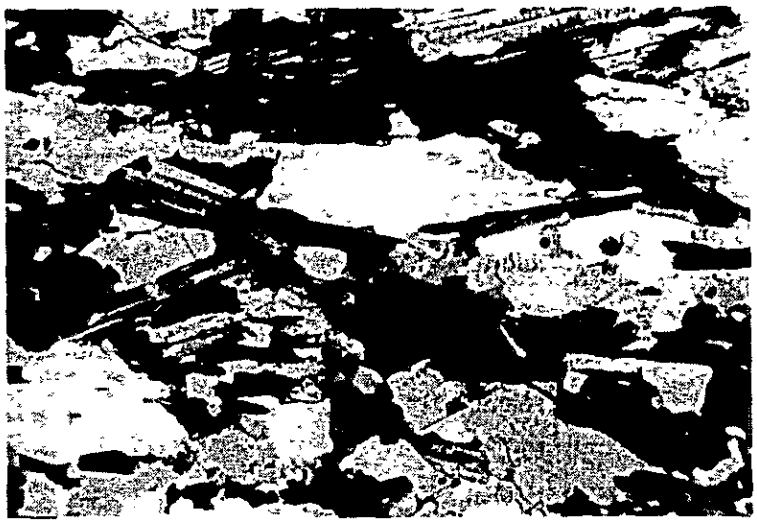

Crossed polars

0 1 mm

Sample No. : 25–1–1
Rock name : Garnet bearing muscovite-biotite gneiss, Juffa gneiss
Locality : West of Wadi Bayt Said, Salalah area
Observation : The rock is holocrystalline and colorless minerals (quartz and plagioclase) and mafic minerals (biotite and muscovite) are alternatively arranged in parallel showing gneissose structure. Garnet, magnetite and apatite are also present as accessoy minerals.

Quartz : Maximum 3 mm, xenomorphic
Plagioclase : Maximum 1.5 mm, hypidiomorphic ~ xenomorphic.
Biotite : Maximum 1 mm, brown, parallel arrangement along gneissose structure.
Muscovite : Maximum 1 mm, parallel arrangement along gneissose structure.
Garnet : Maximum 0.5 mm, associating with biotite.

Photomicrograph 3

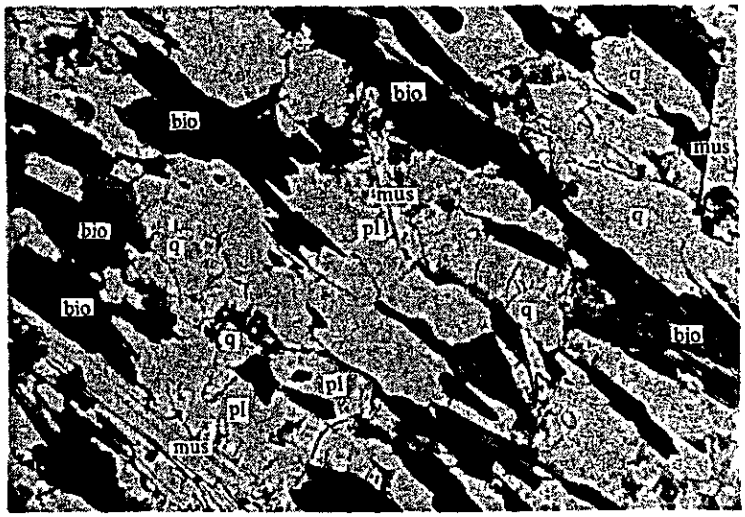

Only lower polar

Photomicrograph 4

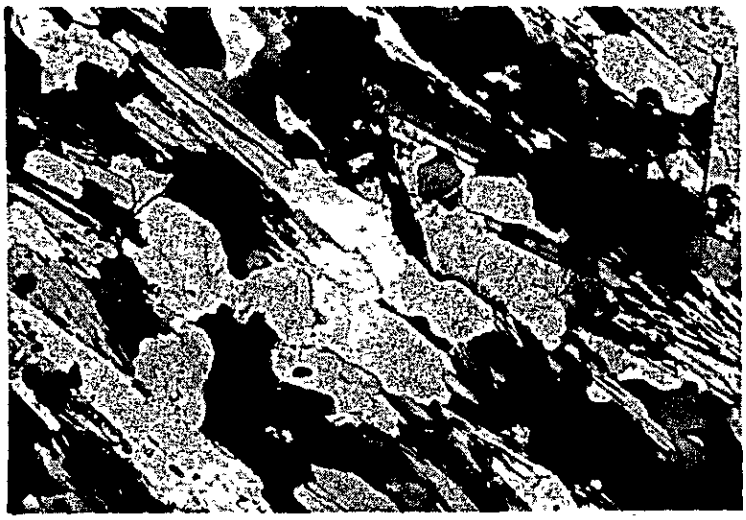

Crossed polars

0 1 mm

Sample No. : 25–2
Rock name : Garnet bearing muscovite-biotite gneiss. Juffa gneiss.
Locality : West of Wadi Bayt Said, Salalah area.
Observation : Same as the photomicrograph 1 and 2.

Photomicrograph 5

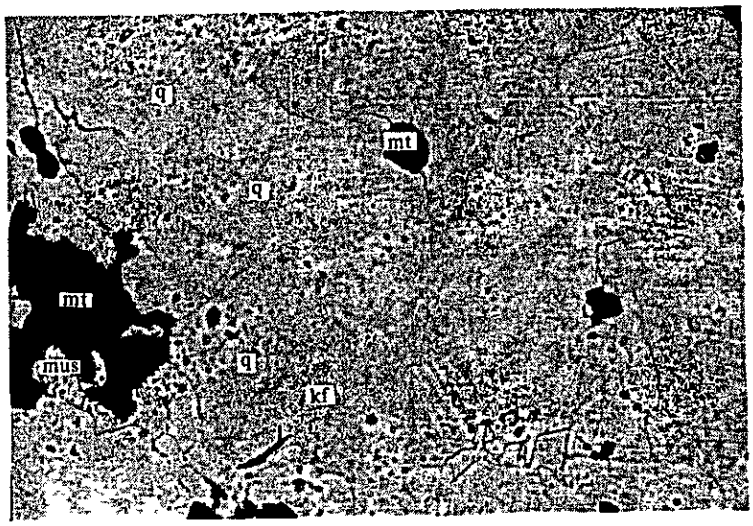

Only lower polar

Photomicrograph 6

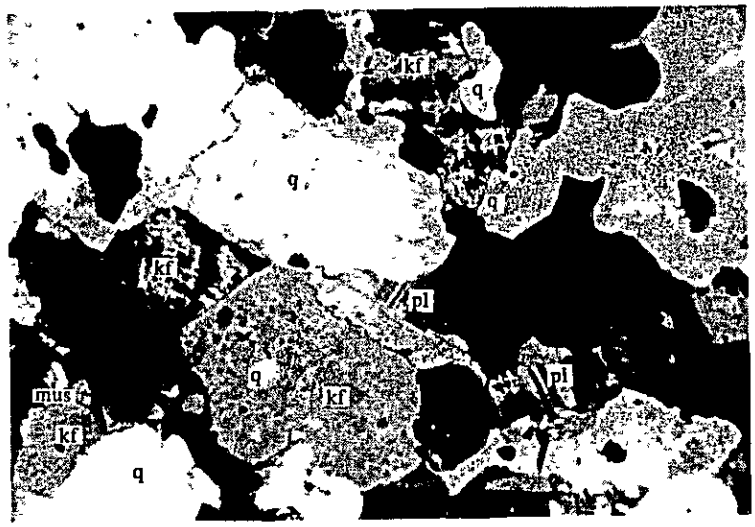

Crossed polars

Sample No. : 22–8
Rock name : Muscovite magnetite injection gneiss, Sadh gneiss
Locality : Near the mouth of Wadi Aingalf
Observation : The rock is holocrystalline and composed of quartz, K-feldspar plagioclase, abundant magnetite, muscovite, biotite and sphene.
Epidote and chlorite are secondary-altered minerals. Small carbonate veins are also recognized.

Quartz : Maximum 2 mm, xenomorphic, many small liquid inclusion.
K-fedspar : Maximum 0.5 mm, xenomorphic, abundant microcline and scarse perthite structures.
Plagioclase : Maximum 2 mm, idiomorphic ~ hypidiomorphic, characteristic albite twinning and alternation to sericite.
Magnetite : Maximum 0.5 mm, distribution along the banded structure.
Muscovite : Maximum 0.5 mm.
Biotite : Maximum 0.5 mm, brown, mostly epidotized and chloritized.

Photomicrograph 7

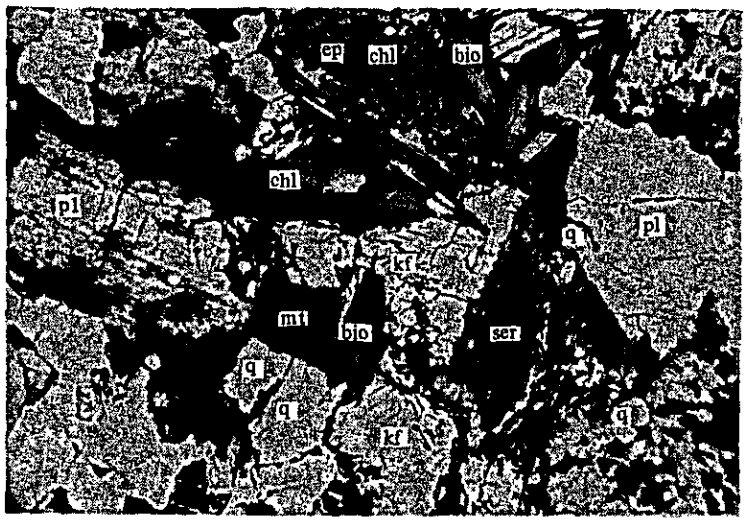

Only lower polar

Photomicrograph 8

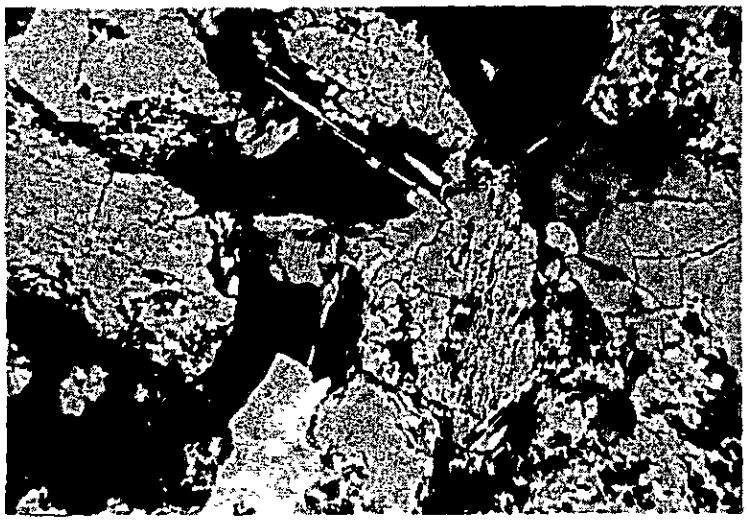

Crossed polars

0 1mm

Sample No. : 27–A–103
Rock name : Gneissose biotite quartz diorite, Sadh gneiss.
Locality : Near the mouth of Wadi Shiliyarn, Salalah area.
Observation : The rock is holocrystaline and composed of plagioclase, quartz, K-feldspar and biotite, and sphene and magnetite are present as accessory minerals.

Plagioclase : Maximum 5 mm, xenomorphic ~ hypidiomorphic. Sericitized, epidotized and zoicitized in some parts.
Quartz : Maximum 0.5 mm, xenomorphic
K-feldspar : Maximum 0.6 mm, xenomorphic ~ hypidiomorphic
Biotite : Maximum 1 mm, idiomorphic, arranged nearly parallel, somewhat chloritized and epidotized.

Photograph 9

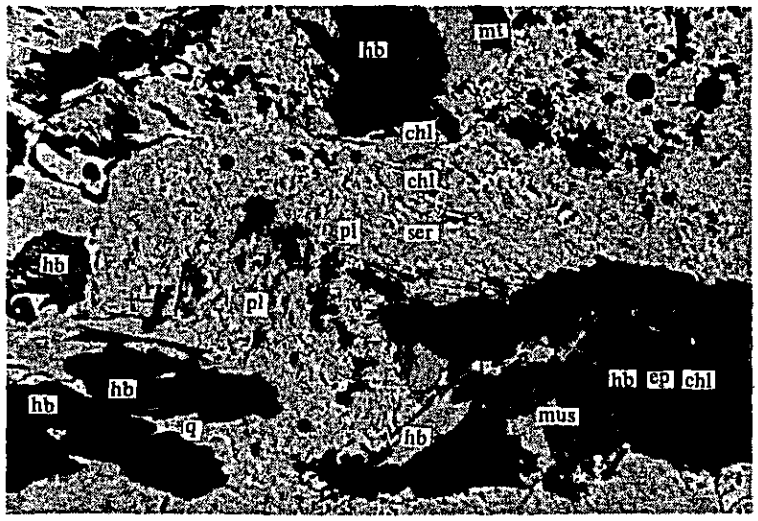

Only lower polar

Photomicrograph 10

Crossed polars

0 1 mm

Sample No. : 28–A–104
Rock name : Gneissose hornblende quartz diorite, Sadh gneiss.
Locality : Wadi Jish Jesh, Salalah area.
Observation : The rock is holocrystalline and composed of plagioclase, quartz, hornblende as well as accessory magnetite and sphene showing gneissose structure. Abundant secondary minerals such as sericite, muscovite, epidote, chlorite, ziocite and goethite are produced.
Plagioclase : Maximum 5 mm, hypidiomorphic, sericitized in some parts.
Hornblende: Maximum 5 mm, green ~ yellowish green, mostly epidotized, zoicitized and chloritized.
Quartz : Maximum 2 mm, xenomorphic.
Magnetite : Some altered to reddish goethite.
Sphene : Associated with hornblende and magnetite.

Photomicrograph 11

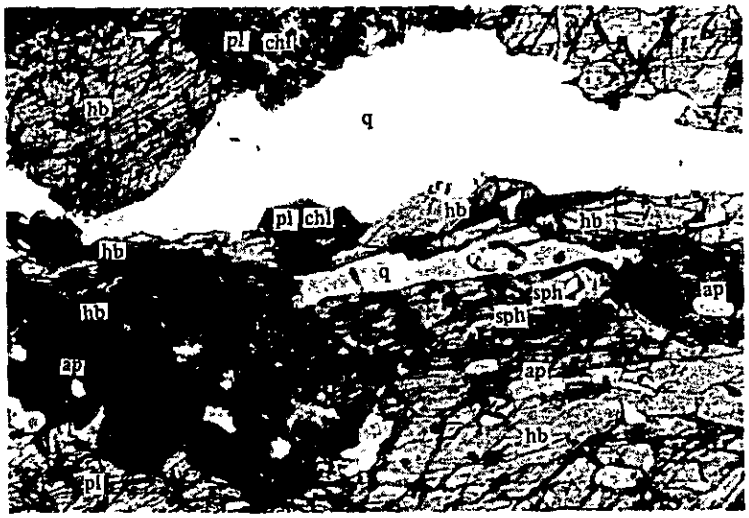

Only lower polar

Photomicrograph 12

Crossed polars

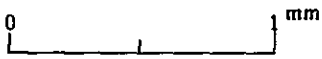

Sample No. : 28–A–109
Rock name : Hornblende gneiss, Sadh gneiss.
Locality : West of Wadi Shaat, Salalah area.
Observation : The rock is holocrystalline and composed of abundant hornblende, plagioclase, quartz as well as accessory magnetite, sphene and apatite.
Hornblende: Maximum 3.5 mm, green to light green, hypidiomorphic, parallel-arranged.
Plagioclase : Maximum 1 mm, xenomorphic, wholly sericitized and epidotized.
Quartz : Maximum 2 mm, xenomorphic, intercalated between the parallel arranged hornblende crystal.
Magnetite : enclosed in hornblende crystals.
Sphene : enclosed in hornblende crystals.
Apatite : enclosed in hornblende crystals.

Photomicrograph 13

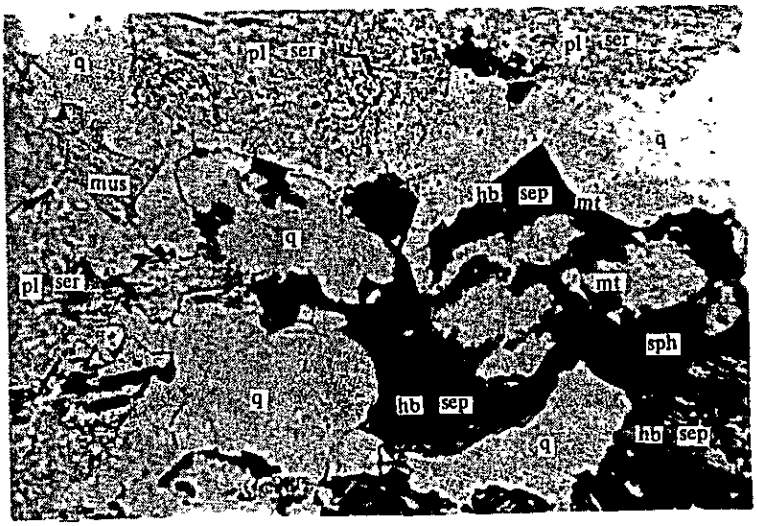

Only lower polar

Photomicrograph 14

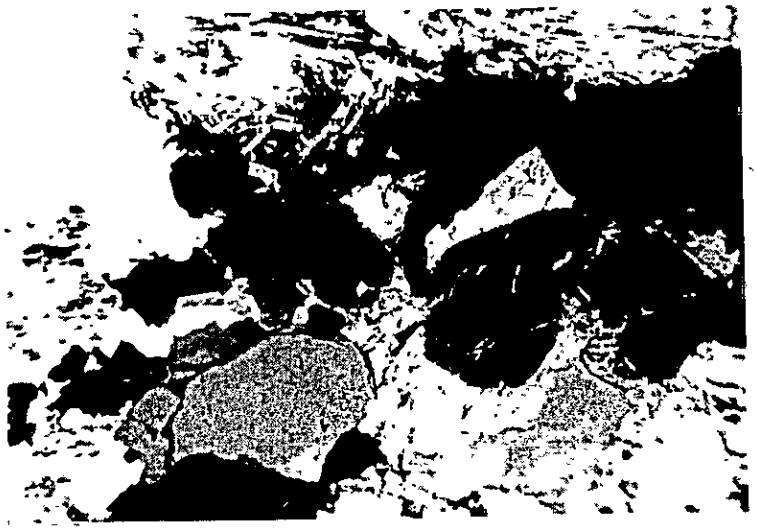

Crossed polars

0 1 mm

Sample No. : 28–A–110
Rock name : Hornblende gneiss, Sadh gneiss.
Locality : Wadi Ayn, Salalah area.
Observation : The rock is holocrystalline and composed of abundant hornblende, plagioclase and quartz as well as accessory magnetite, sphene and apatite.
Hornblende: Maximum 3 mm, green to yellowish green, hypidiomorphic, parallel-arrangement, serpentinized in some parts.
Plagioclase : Maximum 2 mm, hypidiomorphic ~ xenomorphic, mostly sericitized.
Quartz : Maximum 3 mm, xenomorphic.
Sphene : Associated with magnetite and hornblende.
Apatite : Enclosed in hornblende.

Photomicrograph 15

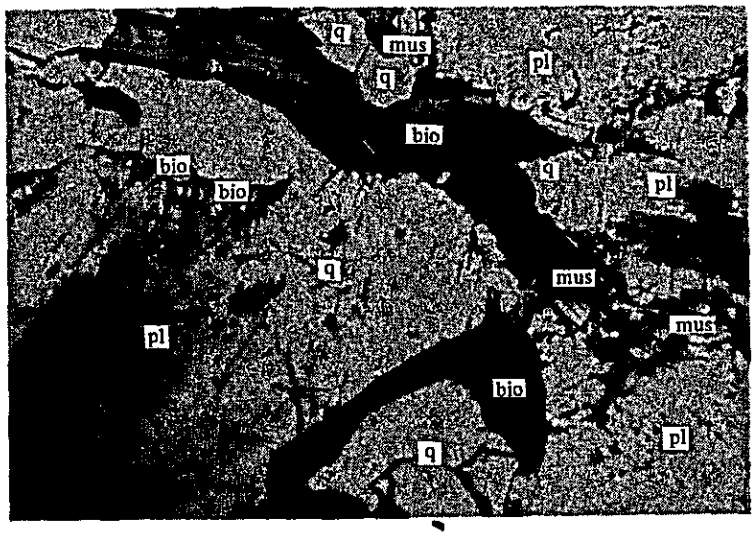

Only lower polar

Photomicrograph 16

Crossed polars

0 1 mm

Sample No. : 22–3–1
Rock name : Muscovite biotite quartz diorite
Locality : The middle part of escarpment of eastern Jabal Samhan, Salalah area.
Observation : The rock is medium-grained and holocrystalline and composed of quartz, plagioclase, and biotite as well as accessory K-feldspar, muscovite, sphene and magnetite. Some parts are altered to sericite, epidote and chlorite.

Quartz : Maximum 8 mm, xenomophic.
Plagioclase : Maximum 5 mm, hypidiomorphic ~ idiomorphic. Some parts sericitized and epidotized.
K-feldspar : Maximum 1 mm, xenomorphic.
Biotite : Maximum 1 mm, hypidiomorphic, brown to yellowish brown, some parts epidotized and chloritized.
Magnetite : Maximum 0.4 mm, associated with and included in biotite, including apatite.

Photomicrograph 17

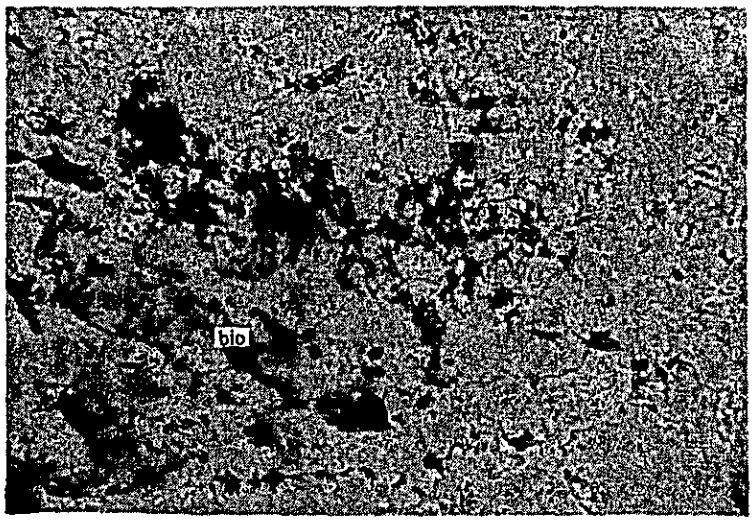

Only lower polar

Photomicrograph 18

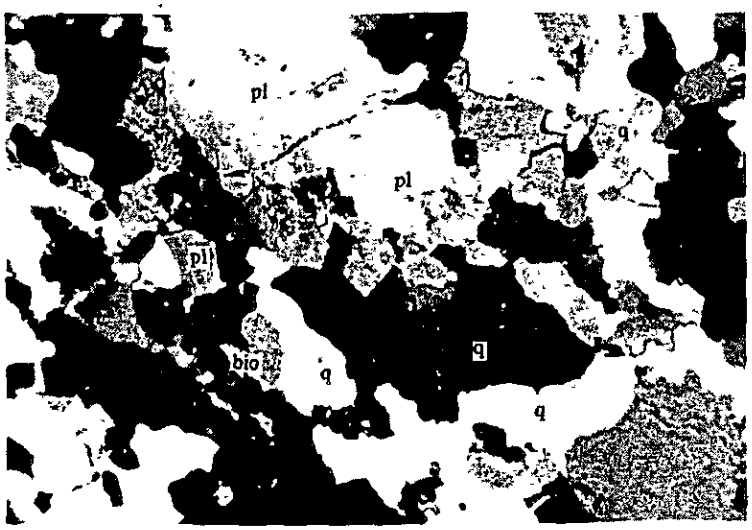

Crossed polars

0 mm

Sample No. : 22–5–1
Rock name : Trondjemite
Locality : About 12 km south of Hasik, Salalah area.
Observation : The rock is holocrystalline and composed of abundant quartz and plagioclase and a very small amount of muscovite and biotite. Some parts are altered to chlorite and epidote.
Quartz : Maximum 6 mm, xenomorphic, including liquid and gas inclusions, some showing mosaic structure.
Plagioclase : Maximum 5 mm, xenomorphic.
Muscovite : Maximum 1 mm.
Biotite : Maximum 1 mm, brown to light brown some parts chloritized and epidotized.

Photomicrograph 19

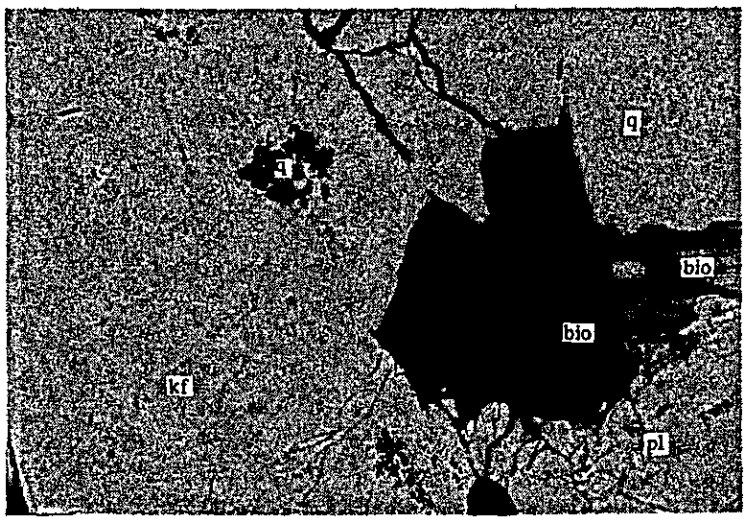

Only lower polar

Photomicrograph 20

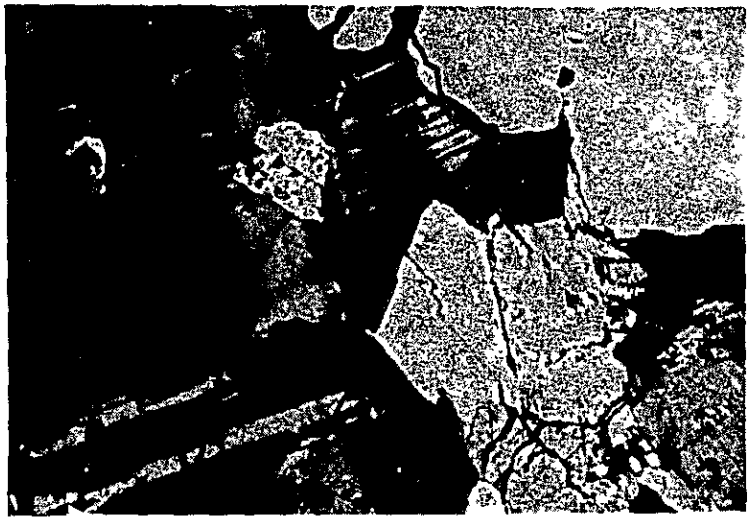

Crossed polars

0 1 mm

Sample No. : 22–6
Rock name : Muscovite biotite granodiorite.
Locality : Ridge west of Wadi Hadabin upstream, Salalah area.
Observation : The rock is holocrystalline, equigranular and composed of quartz, K-feldspar plagioclase and a small amount of biotite and muscovite as well as accessory magnetite and sphene. Carbonate veinlets are present. Some parts are altered to sericite, chlorite and epidote.

Quartz : Maximum 5 mm, xenomorphic.
K-feldspar : Maximum 5 mm, hypidiomorphic, microcline structure.
Plagioclase : Maximum 4 mm, hypidiomorphic, much sericitized.
Biotite : Maximum 1.2 mm, idiomorphic ~ hypidiomorphic, brown to light brown, some parts chloritized and epidotized.

Photomicrograph 21

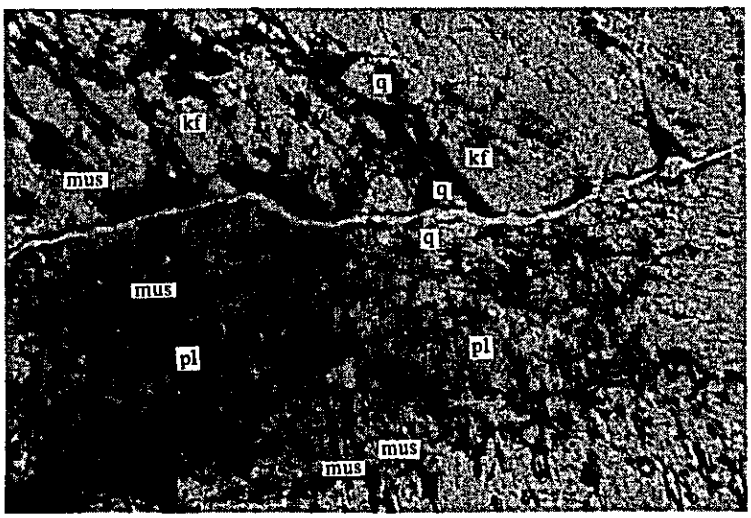

Only lower polar

Photomicrograph 22

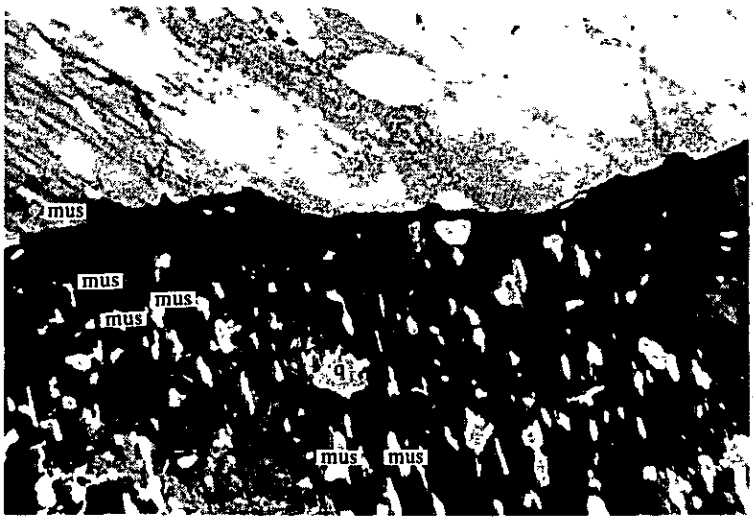

Crossed polars

0 1 mm

Sample No. : 27–A–105
Rock name : Muscovite-plagioclase-quartz-perthite pegmatite.
Locality : Wadi Morir, Salalah area.
Observation : The rock is very coarse-grained and composed of quartz, perthite plagioclase and muscovite. Huge crystals of potash fedspar with perthite structure are present.

Photomicrograph 23

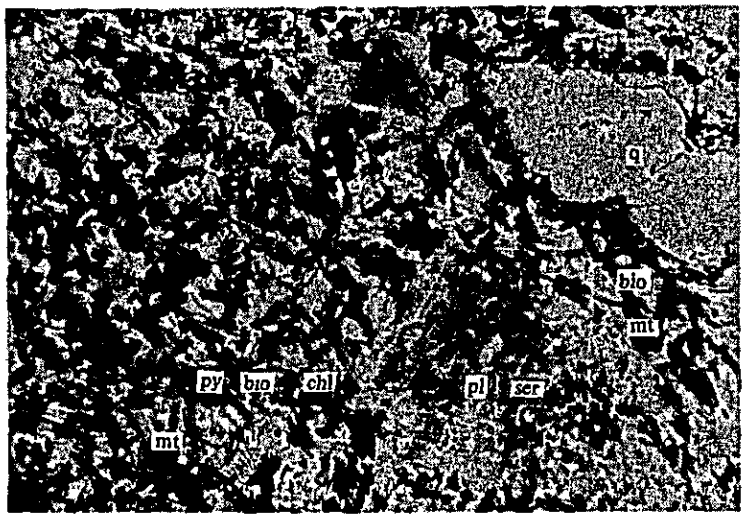

Only lower polar

Photomicrograph 24

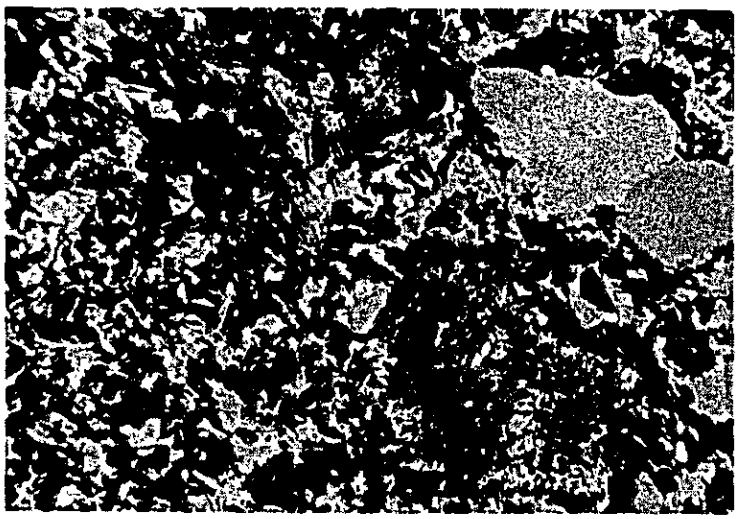

Crossed polars

0 1 mm

Sample No. : 26–A–103
Rock name : Biotite augite quartz dolerite.
Locality : 3 km SE of Wadi Shaat camp site, Salalah area.
Observation : The rock is holocrystalline and has porphyritic texture. Phenocryst is composed of plagioclase (maximum 4 mm) quartz (maximum 2 mm) and chloritized pyroxene (maximum 2 mm). Groundmass is composed of plagioclase lath, monoclinic pyroxene, biotite flakes, quartz and magnetite.
These groundmass minerals show intergranular texture. Carbonitization, sericitization and chloritization are observed and especially, whole pyroxene is altered to chlorite and carbonate.